

CHAPTER 4

PRICING HIGH-DIMENSIONAL AMERICAN CALL OPTIONS

4.1 Introduction

Pricing of high-dimensional options is complicated for American versions of these assets where the owner has the right to exercise early. In this chapter, we use a procedure based on numerical integration and regression for pricing high-dimensional American basket call options where there is a finite, but possibly large, number of exercise dates. The numerical results for the American basket call option prices show that the variation of the prices is not negligible as we vary the non-normality of the underlying distributions in the price process.

4.2 Pricing of American call options on N assets where $N > 2$

Consider an American basket call option on the N assets ($N > 2$) with time T to expiration and a strike price of K . Suppose the distribution of the vector of asset prices $\mathbf{S}(t) = (S_1(t), S_2(t), \dots, S_N(t))$ is described via a Levy process. Let Δt be a small increment in time, $t_k = k \Delta t$, $k = 0, 1, \dots, k^*$, where $k^* \Delta t = T$. The i -th component of the time- t_k value of the vector of asset prices $\mathbf{S}(t_k) = [S_1(t_k), S_2(t_k), \dots, S_N(t_k)]^T$ is then given approximately by

$$S_i(t_k) = S_i^{(k)} \cong S_i^{(k-1)} + S_i^{(k-1)} r \Delta t + S_i^{(k-1)} \sigma_i w_i^{*(k)} \sqrt{\Delta t}, i = 1, 2, \dots, N; \quad k = 0, 1, \dots, k^*.$$

(4.2.1)

Let $a_1 \geq 0, a_2 \geq 0, \dots, a_N \geq 0$ be N given constants such that $a_1 + a_2 + \dots + a_N = 1$,

and

$$h(t_k, \mathbf{x}^{(k)}) = (a_1 S_1(t_k) + a_2 S_2(t_k) + \dots + a_N S_N(t_k) - K)^+ \quad (4.2.2)$$

the payoff from exercise of the basket call option at time t_k at which where $\mathbf{S}(t_k) = \mathbf{x}^{(k)}$, for $k = 0, 1, \dots, k^*$. The conditional-expectation of the option value when $\mathbf{S}(t_{k^*-1}) = \mathbf{x}^{(k^*-1)}$ is given by $E^* [h(t_{k^*}, \mathbf{x}^{(k^*)}) | \mathbf{S}(t_{k^*-1}) = \mathbf{x}^{(k^*-1)}]$ where E^* is as defined in Section 3.2.

For a given risk-free interest rate r , let

$$Q(t_k, \mathbf{x}^{(k)}) = \max(h(t_k, \mathbf{x}^{(k)}), e^{(-r\Delta t)} E^* [Q(t_{k+1}, \mathbf{S}(t_{k+1})) | \mathbf{S}(t_k) = \mathbf{x}^{(k)}]) \text{ for } k < k^* \quad (4.2.3)$$

E^* is as defined in Section 3.2, and

$$Q(t_{k^*}, \mathbf{x}^{(k^*)}) = h(t_{k^*}, \mathbf{x}^{(k^*)}). \quad (4.2.4)$$

The value $Q = Q(0, \mathbf{S}(0))$ will then represent the price of the American basket call option.

The function $Q(t_{k^*}, \mathbf{x}^{(k^*)})$ of $\mathbf{x}^{(k^*)}$ may be computed and summarized as follows.

First we note that the distribution of $\mathbf{S}^{(k^*)}$ (see Section 2.4) is specified by

$$\mathbf{S}^{(k^*)} = \begin{pmatrix} \tilde{\mu}_1^{(k^*)} \\ \vdots \\ \tilde{\mu}_N^{(k^*)} \end{pmatrix} + \tilde{\mathbf{B}}^{(k^*)} \begin{pmatrix} \tilde{\nu}_1^{(k^*)} \\ \vdots \\ \tilde{\nu}_N^{(k^*)} \end{pmatrix} \quad (4.2.5)$$

where

$$\tilde{\nu}_i^{(k^*)} = \begin{cases} \tilde{\lambda}_{i1}^{(k^*)} \tilde{e}_i^{(k^*)} + \tilde{\lambda}_{i2}^{(k^*)} ([\tilde{e}_i^{(k^*)}]^2 - (\frac{1 + \tilde{\lambda}_{i3}^{(k^*)}}{2})), & \tilde{e}_i^{(k^*)} \geq 0 \\ \tilde{\lambda}_{i1}^{(k^*)} \tilde{e}_i^{(k^*)} + \tilde{\lambda}_{i2}^{(k^*)} (\tilde{\lambda}_{i3}^{(k^*)} [\tilde{e}_i^{(k^*)}]^2 - (\frac{1 + \tilde{\lambda}_{i3}^{(k^*)}}{2})), & \tilde{e}_i^{(k^*)} < 0 \end{cases} \quad (4.2.6)$$

and $\tilde{e}_i^{(k^*)} \sim N(0, 1)$, $i=1, 2, \dots, N$.

We transform $(\tilde{e}_1^{(k^*)}, \tilde{e}_2^{(k^*)}, \dots, \tilde{e}_N^{(k^*)})$ to an N -dimensional polar coordinate system given by the radial distance $\tilde{\rho}^{(k^*)}$ and $(N-1)$ polar angles. For example, in the 3-dimensional case, we introduce a spherical coordinate system given by

$$[\tilde{e}_1^{(k^*)}]^2 + [\tilde{e}_2^{(k^*)}]^2 + [\tilde{e}_3^{(k^*)}]^2 = [\tilde{\rho}^{(k^*)}]^2 \quad (4.2.7)$$

$$\tilde{e}_1^{(k^*)} = \tilde{\rho}^{(k^*)} \cos \tilde{\phi}^{(k^*)} \sin \tilde{\theta}^{(k^*)} \quad (4.2.8)$$

$$\tilde{e}_2^{(k^*)} = \tilde{\rho}^{(k^*)} \sin \tilde{\phi}^{(k^*)} \sin \tilde{\theta}^{(k^*)} \quad (4.2.9)$$

and
$$\tilde{e}_3^{(k^*)} = \tilde{\rho}^{(k^*)} \cos \tilde{\theta}^{(k^*)} \quad (4.2.10)$$

for $0^\circ \leq \tilde{\phi}^{(k^*)} \leq 360^\circ$, $0^\circ \leq \tilde{\theta}^{(k^*)} \leq 180^\circ$.

We may also express Eq.(4.2.7)-(4.2.10) as

$$[\tilde{e}_1^{(k^*)}]^2 + [\tilde{e}_2^{(k^*)}]^2 + [\tilde{e}_3^{(k^*)}]^2 = [\tilde{\rho}^{(k^*)}]^2 \quad (4.2.11)$$

$$\tilde{e}_1^{(k^*)} = q_1 \tilde{\rho}^{(k^*)} \cos \tilde{\phi}^{(k^*)} \sin \tilde{\theta}^{(k^*)} \quad (4.2.12)$$

$$\tilde{e}_2^{(k^*)} = q_2 \tilde{\rho}^{(k^*)} \sin \tilde{\phi}^{(k^*)} \sin \tilde{\theta}^{(k^*)} \quad (4.2.13)$$

and
$$\tilde{e}_3^{(k^*)} = q_3 \tilde{\rho}^{(k^*)} \cos \tilde{\theta}^{(k^*)}, 0^\circ \leq \tilde{\phi}^{(k^*)} \leq 90^\circ, 0^\circ \leq \tilde{\theta}^{(k^*)} \leq 90^\circ \quad (4.2.14)$$

where q_1 , q_2 , q_3 (see Table 4.2.1) depend on the quadrant in which the point

$(\tilde{e}_1^{(k^*)}, \tilde{e}_2^{(k^*)}, \tilde{e}_3^{(k^*)})$ lies.

Table 4.2.1: The values of q_1 , q_2 , q_3

Quadrant No.	q_1	q_2	q_3
1	1	1	1
2	1	1	-1
3	1	-1	1
4	1	-1	-1
5	-1	1	1
6	-1	1	-1
7	-1	-1	1
8	-1	-1	-1

In general, for the N-dimensional case, we can express $\tilde{\epsilon}_1^{(k^*)}$ as follows:

$$[\tilde{\epsilon}_1^{(k^*)}]^2 + [\tilde{\epsilon}_2^{(k^*)}]^2 + \dots + [\tilde{\epsilon}_N^{(k^*)}]^2 = [\tilde{\rho}^{(k^*)}]^2 \quad (4.2.15)$$

$$\tilde{\epsilon}_1^{(k^*)} = q_1 \tilde{\rho}^{(k^*)} \cos \tilde{\theta}_{N-1}^{(k^*)} \cos \tilde{\theta}_{N-2}^{(k^*)} \cos \tilde{\theta}_{N-3}^{(k^*)} \dots \cos \tilde{\theta}_2^{(k^*)} \sin \tilde{\theta}_1^{(k^*)} \quad (4.2.16)$$

$$\tilde{\epsilon}_2^{(k^*)} = q_2 \tilde{\rho}^{(k^*)} \sin \tilde{\theta}_{N-1}^{(k^*)} \cos \tilde{\theta}_{N-2}^{(k^*)} \cos \tilde{\theta}_{N-3}^{(k^*)} \dots \cos \tilde{\theta}_2^{(k^*)} \sin \tilde{\theta}_1^{(k^*)} \quad (4.2.17)$$

$$\tilde{\epsilon}_3^{(k^*)} = q_3 \tilde{\rho}^{(k^*)} \sin \tilde{\theta}_{N-2}^{(k^*)} \cos \tilde{\theta}_{N-3}^{(k^*)} \dots \cos \tilde{\theta}_2^{(k^*)} \sin \tilde{\theta}_1^{(k^*)} \quad (4.2.18)$$

⋮

$$\tilde{\epsilon}_{N-1}^{(k^*)} = q_{N-1} \tilde{\rho}^{(k^*)} \sin \tilde{\theta}_2^{(k^*)} \sin \tilde{\theta}_1^{(k^*)} \quad (4.2.19)$$

$$\tilde{\epsilon}_N^{(k^*)} = q_N \tilde{\rho}^{(k^*)} \cos \tilde{\theta}_1^{(k^*)}, 0^\circ \leq \tilde{\theta}_i^{(k^*)} \leq 90^\circ, i = 1, 2, \dots, N-1 \quad (4.2.20)$$

where $q_i = -1$ or $+1$ for $i = 1, 2, \dots, N$.

For each of the 2^N quadrants, we choose randomly a set of n_r values of $\tilde{\Theta}^{(k^*)} = (\tilde{\theta}_1^{(k^*)}, \tilde{\theta}_2^{(k^*)}, \dots, \tilde{\theta}_{N-1}^{(k^*)})$, and for each chosen value of $\tilde{\Theta}^{(k^*)}$, we consider the following n_r+1 values of $\tilde{\rho}^{(k^*)}$:

$$\tilde{\rho}_j^{(k^*)} = jh, j=0, 1, \dots, n_r \quad (4.2.21)$$

where $h = \phi/n_r$ and $\phi^2 = \chi_{N,0.01}^2$ is the 99% point of the chi square distribution with N degrees of freedom. For each $\tilde{\Theta}^{(k^*)}$, we use Eq.(4.2.2) and Eq.(4.2.4) - (4.2.6) to find $Q(t_{k^*}, \mathbf{x}^{(k^*)})$ as a function of $\tilde{\rho}^{(k^*)}$. This function of $\tilde{\rho}^{(k^*)}$ turns out to be the form

$$Q(t_{k^*}, \mathbf{x}^{(k^*)}) \equiv \begin{cases} Q_1(t_{k^*}, \mathbf{x}^{(k^*)}) & \text{for } 0 \leq \tilde{\rho}^{(k^*)} \leq \tilde{\xi}^{(k^*)} \\ 0 & \text{for } \tilde{\rho}^{(k^*)} > \tilde{\xi}^{(k^*)} \end{cases} \quad (4.2.22)$$

where $\tilde{\xi}^{(k^*)}$ is a constant which depends on $\tilde{\Theta}^{(k^*)}$.

We may approximate $Q(t_{k^*}, \mathbf{x}^{(k^*)})$ by a quadratic function of $\tilde{\rho}^{(k^*)}$ and express $Q(t_{k^*}, \mathbf{x}^{(k^*)})$ as

$$Q(t_{k^*}, \mathbf{x}^{(k^*)}) = \begin{cases} \tilde{c}_0^{(k^*)} + \tilde{c}_1^{(k^*)}\tilde{\rho}^{(k^*)} + \tilde{c}_2^{(k^*)}[\tilde{\rho}^{(k^*)}]^2, & 0 \leq \tilde{\rho}^{(k^*)} \leq \tilde{\xi}^{(k^*)} \\ 0, & \tilde{\rho}^{(k^*)} > \tilde{\xi}^{(k^*)} \end{cases} \quad (4.2.23)$$

where $\tilde{c}_0^{(k^*)}$, $\tilde{c}_1^{(k^*)}$, $\tilde{c}_2^{(k^*)}$ and $\tilde{\xi}^{(k^*)}$ are constants which depend on $\tilde{\Theta}^{(k^*)}$.

For example, consider the case when $N=3$, $T=10/365$, $r=0.05$, $K=46$, $a_1 = 0.3$, $a_2 = 0.3$, and $a_3 = 0.4$. Let $\bar{m}_3^{(i)} = E[v_i^{(k)}]^3$ and $\bar{m}_4^{(i)} = E[v_i^{(k)}]^4$ (see Eq.(2.4.2)). Suppose the (i, j) entry of $\mathbf{P} = \{\text{corr}(w_i^{(k)}, w_j^{(k)})\}$ is given by Table 4.2.2 and the values of $\mu_i, \sigma_i, \mathbf{S}^{(0)}$, $\bar{m}_3^{(i)}$ and $\bar{m}_4^{(i)}$ are given by Table 4.2.3 for $i, j = 1, 2, 3$.

Table 4.2.2: The (i, j) entry of $\mathbf{P} = \{\text{corr}(w_i^{(k)}, w_j^{(k)})\}$

		j		
		1	2	3
i	1	1	0.1	0.15
	2	0.1	1	0.05
	3	0.15	0.05	1

Table 4.2.3: Values of $\mu_i, \sigma_i, \mathbf{S}^{(0)}$, $\bar{m}_3^{(i)}$ and $\bar{m}_4^{(i)}$

[$N=3$, exercise dates are $1/365, 2/365, \dots, 10/365$, $r=0.05$, $K=46$, $a_1 = 0.3$, $a_2 = 0.3$, and $a_3 = 0.4$]

i	μ_i	σ_i	$\mathbf{S}^{(0)}$	$\bar{m}_3^{(i)}$	$\bar{m}_4^{(i)}$
1	0.05	0.15	50	0.1	5.0
2	0.05	0.1	60	0.2	4.0
3	0.05	0.2	35	0.2	3.8

Examples of the fitted quadratic function of $Q(t_{k^*}, \mathbf{x}^{(k^*)})$ are shown in Figures 4.2.1 – 4.2.2. Figures 4.2.1 – 4.2.2 show that the right side of Eq.(4.2.23) gives a satisfactory fit to the computed values of $Q(t_{k^*}, \mathbf{x}^{(k^*)})$.

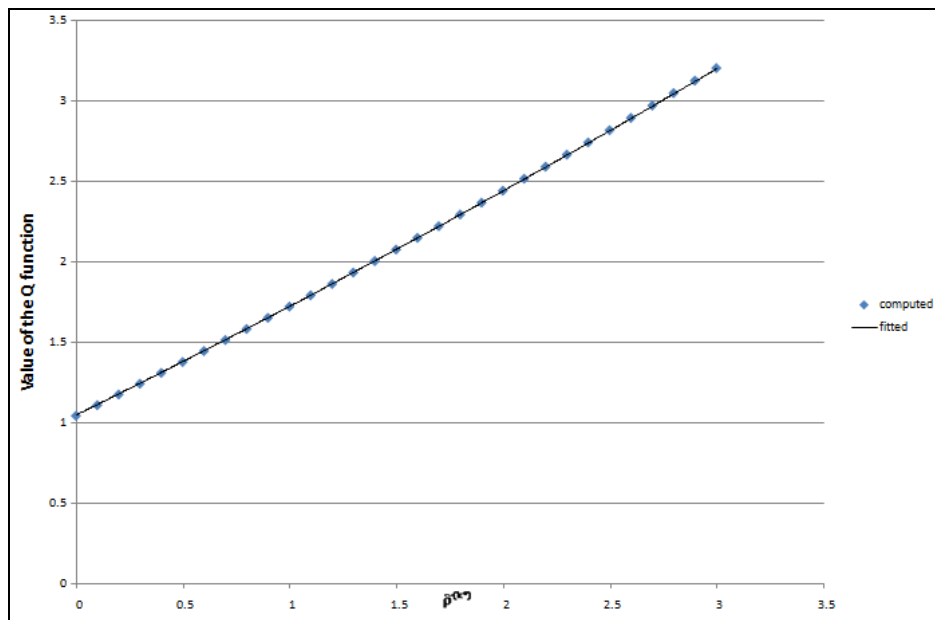


Figure 4.2.1: Computed and fitted values of $Q(t_{k^*}, \mathbf{x}^{(k^*)})$

[N=3, Quadrant number=1, exercise dates are 1/365, 2/365, ..., 10/365, $r=0.05$, $K=46$,

$$(\tilde{\theta}_1^{(k^*)}, \tilde{\theta}_2^{(k^*)}) = (0^\circ, 0^\circ), (n_v, n_r) = (20, 30), \text{ fitted function is}$$

$y = 0.02089x^2 + 0.65561x + 1.04905$, other parameters are as given in Tables 4.2.2 and 4.2.3]

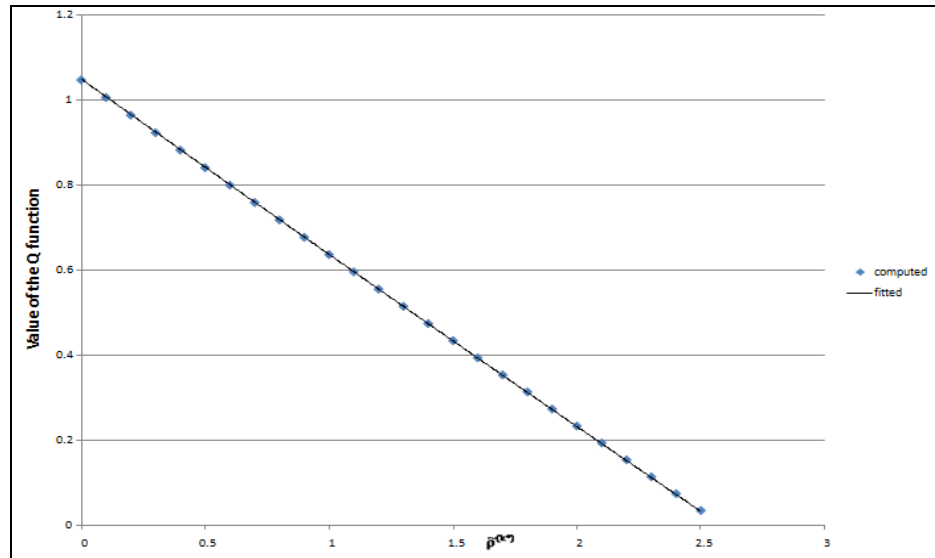


Figure 4.2.2: Computed and fitted values of $Q(t_{k^*}, \mathbf{x}^{(k^*)})$

[N=3, Quadrant number=8, exercise dates are 1/365, 2/365, ..., 10/365, $r=0.05$, $K=46$,

$$(\tilde{\theta}_1^{(k^*)}, \tilde{\theta}_2^{(k^*)}) = (74^\circ, 11^\circ), (n_v, n_r) = (20, 30), \text{ fitted function is } y = 0.003835x^2 -$$

$0.41564x + 1.04905$, other parameters are as given in Tables 4.2.2 and 4.2.3]

Then, for each quadrant and each value of $g = 0, 1, 2$, we may regress $\tilde{c}_g^{(k^*)}$ on

$\tilde{\theta}_1^{(k^*)}, \tilde{\theta}_2^{(k^*)}, \dots, \tilde{\theta}_{N-1}^{(k^*)}$ to get

$$\tilde{c}_g^{(k^*)} = \tilde{d}_{g0}^{(k^*)} + \sum_{i=1}^{N-1} \tilde{d}_{gi}^{(k^*)} \tilde{\theta}_i^{(k^*)} + \sum_{\substack{i=1 \\ i \neq j}}^{N-1} \sum_{j=1}^{N-1} \tilde{d}_{gij}^{(k^*)} \tilde{\theta}_i^{(k^*)} \tilde{\theta}_j^{(k^*)} + \sum_{i=1}^{N-1} \tilde{d}_{gii}^{(k^*)} [\tilde{\theta}_i^{(k^*)}]^2, \quad (4.2.24)$$

for $0^\circ \leq \tilde{\theta}_i^{(k^*)} \leq 90^\circ$, $i, j = 1, 2, \dots, N-1$.

Examples of the computed and fitted value of $\tilde{c}_g^{(k^*)}$, $g = 0, 1, 2$, in the first and fourth quadrants with $(n_v, n_r) = (20, 30)$ when $N = 3$ are shown in Figures 4.2.3 – 4.2.8. The figures indicate that the fit given by Eq.(4.2.24) seems to be satisfactory as the plot of the computed value and the fitted value of $\tilde{c}_g^{(k^*)}$ cluster around the straight line $y = x$.

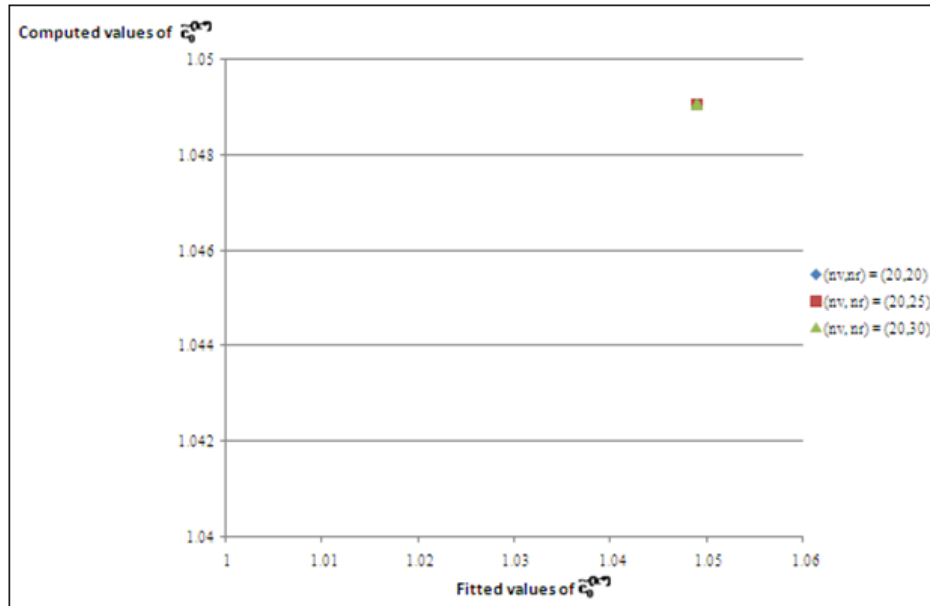


Figure 4.2.3: The fitted and computed values of the coefficient $\tilde{c}_0^{(k^*)}$ of $Q(t_{k^*}, \mathbf{x}^{(k^*)})$

[$N=3$, Quadrant number=1, exercise dates are $1/365, 2/365, \dots, 10/365$, $r=0.05$, $K=46$, $(n_v, n_r)=(20, 20), (20, 25), (20, 30)$, the fitted equations for $\tilde{c}_0^{(k^*)}$ is

$$\begin{aligned} \tilde{c}_0^{(k^*)} = & 1.0491 - (5.00E - 16)\tilde{\theta}_1^{(k^*)} - (4.44E - 16)\tilde{\theta}_2^{(k^*)} \\ & - (1.30E - 18)\tilde{\theta}_1^{(k^*)}\tilde{\theta}_2^{(k^*)} - (8.67E - 19)[\tilde{\theta}_1^{(k^*)}]^2 + (3.47E - 18)[\tilde{\theta}_2^{(k^*)}]^2, \text{ other parameters are as} \\ & \text{given in Tables 4.2.2 and 4.2.3] \end{aligned}$$

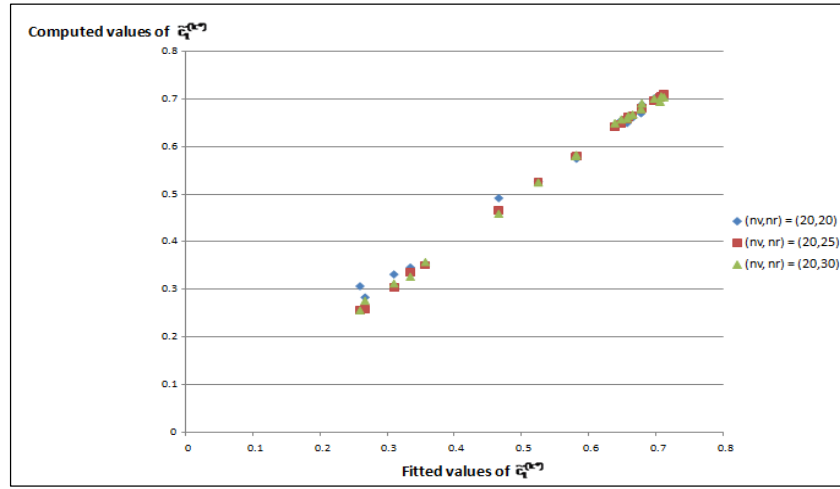


Figure 4.2.4: The fitted and computed values of the coefficient $\tilde{c}_1^{(k^*)}$ of $Q(t_{k^*}, \mathbf{x}^{(k^*)})$

[N=3, Quadrant number=1, exercise dates are 1/365, 2/365, ..., 10/365, $r=0.05$, $K=46$,

$(n_v, n_r)=(20, 20), (20, 25), (20, 30)$, the fitted equations for $\tilde{c}_1^{(k^*)}$ is

$$\begin{aligned} \tilde{c}_1^{(k^*)} = & 0.648 + 0.0032\tilde{\theta}_1^{(k^*)} + 0.0023\tilde{\theta}_2^{(k^*)} \\ & - (1.50E - 06)\tilde{\theta}_1^{(k^*)}\tilde{\theta}_2^{(k^*)} - (8.89E - 05)[\tilde{\theta}_1^{(k^*)}]^2 - (3.21E - 05)[\tilde{\theta}_2^{(k^*)}]^2, \end{aligned}$$

other parameters are as given in Tables 4.2.2 and 4.2.3]

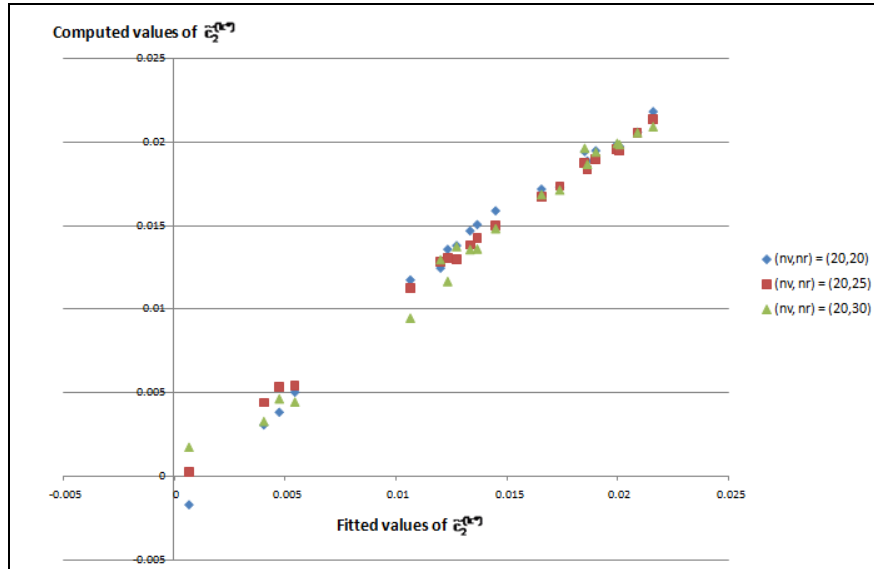


Figure 4.2.5: The fitted and computed values of the coefficient $\tilde{c}_2^{(k^*)}$ of $Q(t_{k^*}, \mathbf{x}^{(k^*)})$

[N=3, Quadrant number=1, exercise dates are 1/365, 2/365, ..., 10/365, $r=0.05$, $K=46$,

$(n_v, n_r)=(20, 20), (20, 25), (20, 30)$, the fitted equations for $\tilde{c}_2^{(k^*)}$ is

$$\begin{aligned} \tilde{c}_2^{(k^*)} = & 0.02159 - (2.57E - 04)\tilde{\theta}_1^{(k^*)} + (1.02E - 05)\tilde{\theta}_2^{(k^*)} \\ & + (1.86E - 06)\tilde{\theta}_1^{(k^*)}\tilde{\theta}_2^{(k^*)} + (1.64E - 07)[\tilde{\theta}_1^{(k^*)}]^2 + (2.07E - 07)[\tilde{\theta}_2^{(k^*)}]^2, \end{aligned}$$

other parameters are as given in Tables 4.2.2 and 4.2.3]

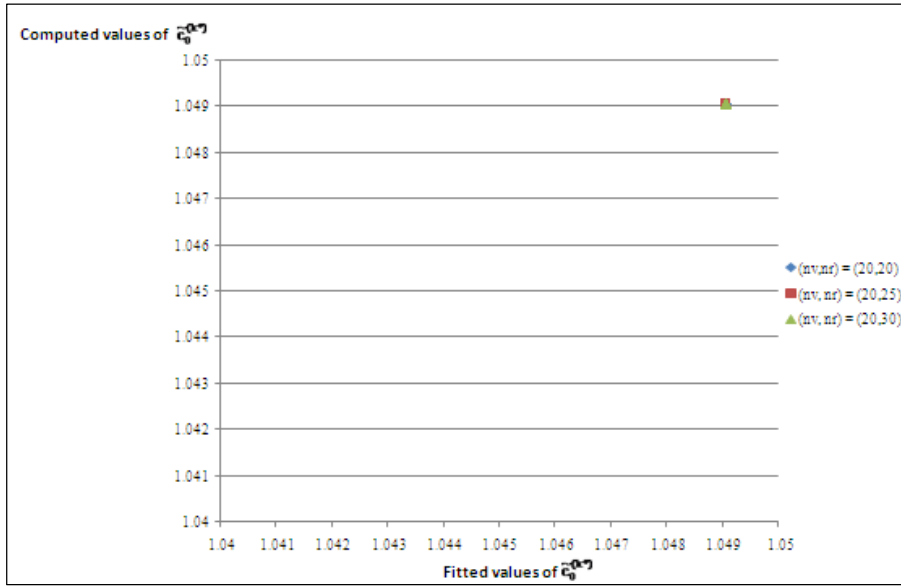


Figure 4.2.6: The fitted and computed values of the coefficient $\tilde{c}_0^{(k^*)}$ of $Q(t_{k^*}, \mathbf{x}^{(k^*)})$

[N=3, Quadrant number=4, exercise dates are 1/365, 2/365, ..., 10/365, $r=0.05$, K=46, $(n_v, n_r)=(20, 20), (20, 25), (20, 30)$, the fitted equations for $\tilde{c}_0^{(k^*)}$ is

$$\begin{aligned} \tilde{c}_0^{(k^*)} = & 1.049 + (0E+00)\tilde{\theta}_1^{(k^*)} - (2.22E-16)\tilde{\theta}_2^{(k^*)} \\ & + (0.E+00)\tilde{\theta}_1^{(k^*)}\tilde{\theta}_2^{(k^*)} - (3.93E-19)[\tilde{\theta}_1^{(k^*)}]^2 + (0E+00)[\tilde{\theta}_2^{(k^*)}]^2, \text{ other parameters are as} \\ & \text{given in Tables 4.2.2 and 4.2.3] \end{aligned}$$

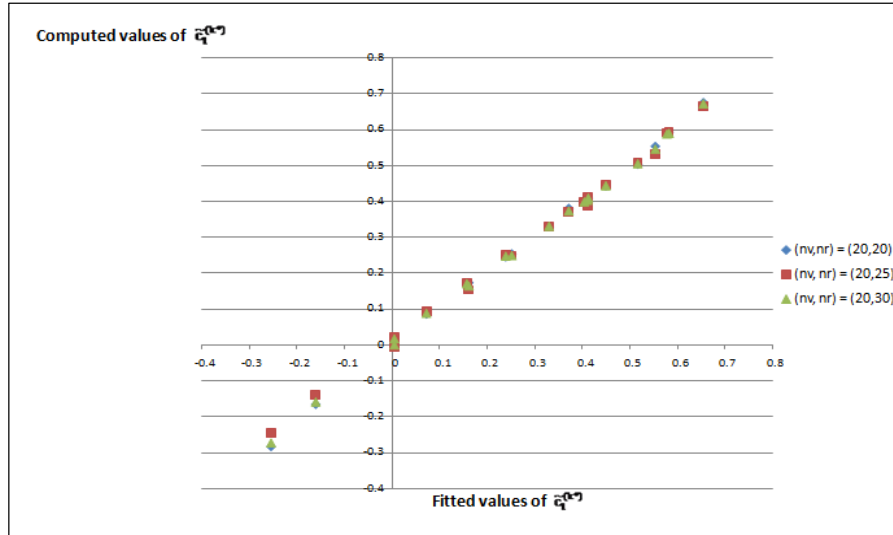


Figure 4.2.7: The fitted and computed values of the coefficient $\tilde{c}_1^{(k^*)}$ of $Q(t_{k^*}, \mathbf{x}^{(k^*)})$

[N=3, Quadrant number=4, exercise dates are 1/365, 2/365, ..., 10/365, $r=0.05$, K=46, $(n_v, n_r)=(20, 20), (20, 25), (20, 30)$, the fitted equations for $\tilde{c}_1^{(k^*)}$ is

$$\begin{aligned} \tilde{c}_1^{(k^*)} = & 0.6698 - 0.00598\tilde{\theta}_1^{(k^*)} - 0.00143\tilde{\theta}_2^{(k^*)} - (1.52E-06)\tilde{\theta}_1^{(k^*)}\tilde{\theta}_2^{(k^*)} \\ & - (4.85E-05)[\tilde{\theta}_1^{(k^*)}]^2 + (2.29E-05)[\tilde{\theta}_2^{(k^*)}]^2, \text{ other parameters are as given in Tables} \\ & \text{4.2.2 and 4.2.3] \end{aligned}$$

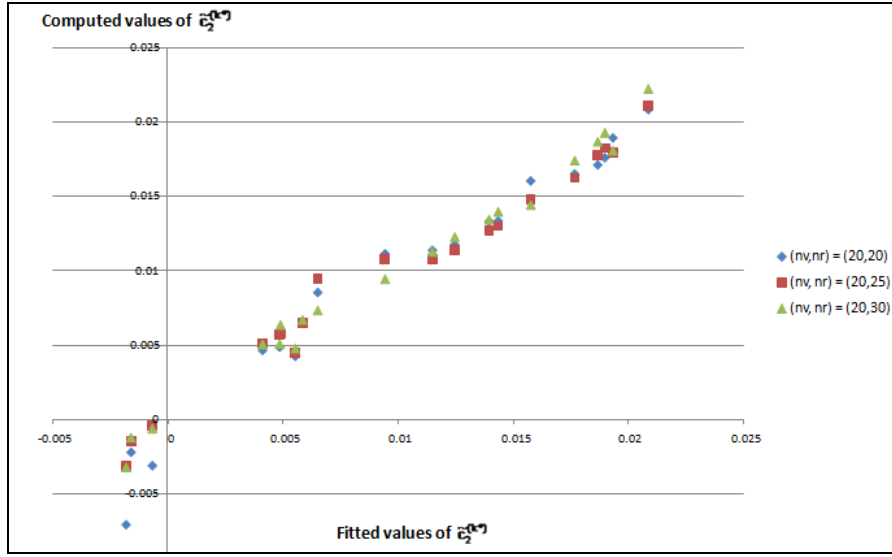


Figure 4.2.8: The fitted and computed values of the coefficient $\tilde{c}_2^{(k^*)}$ of $Q(t_{k^*}, \mathbf{x}^{(k^*)})$

[$N=3$, Quadrant number=4, exercise dates are 1/365, 2/365, ..., 10/365, $r=0.05$, $K=46$,

$(n_v, n_r)=(20, 20), (20, 25), (20, 30)$, the fitted equations for $\tilde{c}_2^{(k^*)}$ is

$$\begin{aligned} \tilde{c}_2^{(k^*)} = & 0.0223 - (2.45E-04)\tilde{\theta}_1^{(k^*)} + (1.01E-04)\tilde{\theta}_2^{(k^*)} - (3.20E-06)\tilde{\theta}_1^{(k^*)}\tilde{\theta}_2^{(k^*)} \\ & + (5.20E-07)[\tilde{\theta}_1^{(k^*)}]^2 - (7.31E-07)[\tilde{\theta}_2^{(k^*)}]^2, \text{ other parameters are as given in Tables} \\ & \text{4.2.2 and 4.2.3]} \end{aligned}$$

For $k = k^*, k^* - 1, \dots, 2, 1$, we next find $Q(t_{k-1}, \mathbf{x}^{(k-1)})$. To achieve this, we first note

that the distribution of $\mathbf{S}^{(k-1)}$ can be described via

$$\mathbf{S}^{(k-1)} = \begin{pmatrix} \tilde{\mu}_1^{(k-1)} \\ \vdots \\ \tilde{\mu}_N^{(k-1)} \end{pmatrix} + \tilde{\mathbf{B}}^{(k-1)} \begin{pmatrix} \tilde{v}_1^{(k-1)} \\ \vdots \\ \tilde{v}_N^{(k-1)} \end{pmatrix} \quad (4.2.25)$$

where

$$\tilde{v}_i^{(k-1)} = \begin{cases} \tilde{\lambda}_{i1}^{(k-1)}\tilde{e}_i^{(k-1)} + \tilde{\lambda}_{i2}^{(k-1)}([\tilde{e}_i^{(k-1)}]^2 - (\frac{1+\tilde{\lambda}_{i3}^{(k-1)}}{2})), & \tilde{e}_i^{(k-1)} \geq 0 \\ \tilde{\lambda}_{i1}^{(k-1)}\tilde{e}_i^{(k-1)} + \tilde{\lambda}_{i2}^{(k-1)}(\tilde{\lambda}_{i3}^{(k-1)}[\tilde{e}_i^{(k-1)}]^2 - (\frac{1+\tilde{\lambda}_{i3}^{(k-1)}}{2})), & \tilde{e}_i^{(k-1)} < 0 \end{cases} \quad (4.2.26)$$

We again introduce an N-dimensional polar coordinate system given by

$$[\tilde{e}_1^{(k-1)}]^2 + [\tilde{e}_2^{(k-1)}]^2 + \dots + [\tilde{e}_N^{(k-1)}]^2 = [\tilde{\rho}^{(k-1)}]^2 \quad (4.2.27)$$

$$\tilde{e}_1^{(k-1)} = q_1 \tilde{\rho}^{(k-1)} \cos \tilde{\theta}_{N-1}^{(k-1)} \cos \tilde{\theta}_{N-2}^{(k-1)} \cos \tilde{\theta}_{N-3}^{(k-1)} \dots \cos \tilde{\theta}_2^{(k-1)} \sin \tilde{\theta}_1^{(k-1)} \quad (4.2.28)$$

$$\tilde{e}_2^{(k-1)} = q_2 \tilde{\rho}^{(k-1)} \sin \tilde{\theta}_{N-1}^{(k-1)} \cos \tilde{\theta}_{N-2}^{(k-1)} \cos \tilde{\theta}_{N-3}^{(k-1)} \dots \cos \tilde{\theta}_2^{(k-1)} \sin \tilde{\theta}_1^{(k-1)} \quad (4.2.29)$$

$$\tilde{e}_3^{(k-1)} = q_3 \tilde{\rho}^{(k-1)} \sin \tilde{\theta}_{N-2}^{(k-1)} \cos \tilde{\theta}_{N-3}^{(k-1)} \dots \cos \tilde{\theta}_2^{(k-1)} \sin \tilde{\theta}_1^{(k-1)} \quad (4.2.30)$$

⋮

$$\tilde{e}_{N-1}^{(k-1)} = q_{N-1} \tilde{\rho}^{(k-1)} \sin \tilde{\theta}_2^{(k-1)} \sin \tilde{\theta}_1^{(k-1)} \quad (4.2.31)$$

$$\tilde{e}_N^{(k-1)} = q_N \tilde{\rho}^{(k-1)} \cos \tilde{\theta}_1^{(k-1)}, \quad (4.2.32)$$

$$0^\circ \leq \tilde{\theta}_i^{(k-1)} \leq 90^\circ, \quad i = 1, 2, \dots, N-1$$

For each of the 2^N quadrants, we choose randomly a set of n_r values of $\tilde{\Theta}^{(k-1)} = (\tilde{\theta}_1^{(k-1)}, \tilde{\theta}_2^{(k-1)}, \dots, \tilde{\theta}_{N-1}^{(k-1)})$, and for each chosen value of $\tilde{\Theta}^{(k-1)}$, we consider the following n_r+1 values of $\tilde{\rho}^{(k-1)}$:

$$\tilde{\rho}_j^{(k-1)} = jh, \quad j=0, 1, \dots, n_r \quad (4.2.33)$$

where $h = \phi/n_r$ and $\phi^2 = \chi_{N,0.01}^2$ is the 99% point of the chi square distribution with N

degrees of freedom. For each $\tilde{\Theta}^{(k-1)}$, we

- (i) find $\tilde{e}_i^{(k-1)}$, for $i=1, 2, \dots, N$ by using Eq.(4.2.28) – (4.2.32) with $\tilde{\rho}^{(k-1)} = \tilde{\rho}_j^{(k-1)}$,
- (ii) find $\tilde{v}_i^{(k-1)}$, for $i=1, 2, \dots, N$ by using Eq.(4.2.26), and
- (iii) find $\mathbf{S}(t_{k-1}) = \mathbf{x}^{(k-1)}$ by using Eq.(4.2.25).

We next need to find $h(t_{k-1}, \mathbf{x}^{(k-1)})$ and $E^*[Q(t_k, \mathbf{S}^{(k)} | \mathbf{S}^{(k-1)} = \mathbf{x}^{(k-1)})]$ in order to determine $Q(t_{k-1}, \mathbf{x}^{(k-1)})$.

To find $E^*[Q(t_k, \mathbf{S}^{(k)} | \mathbf{S}^{(k-1)} = \mathbf{x}^{(k-1)})]$, we may perform an N-dimensional numerical integration. The relevant procedure is as follows.

First we introduce an N-dimensional polar coordinate system given by

$$[e_1^{(k)}]^2 + [e_2^{(k)}]^2 + \dots + [e_N^{(k)}]^2 = [\rho^{(k)}]^2 \quad (4.2.34)$$

$$e_1^{(k)} = q_1 \rho^{(k)} \cos \theta_{N-1}^{(k)} \cos \theta_{N-2}^{(k)} \cos \theta_{N-3}^{(k)} \dots \cos \theta_2^{(k)} \sin \theta_1^{(k)} \quad (4.2.35)$$

$$e_2^{(k)} = q_2 \rho^{(k)} \sin \theta_{N-1}^{(k)} \cos \theta_{N-2}^{(k)} \cos \theta_{N-3}^{(k)} \dots \cos \theta_2^{(k)} \sin \theta_1^{(k)} \quad (4.2.36)$$

$$e_3^{(k)} = q_3 \rho^{(k)} \sin \theta_{N-2}^{(k)} \cos \theta_{N-3}^{(k)} \dots \cos \theta_2^{(k)} \sin \theta_1^{(k)} \quad (4.2.37)$$

⋮

$$e_{N-1}^{(k)} = q_{N-1} \rho^{(k)} \sin \theta_2^{(k)} \sin \theta_1^{(k)} \quad (4.2.38)$$

$$e_N^{(k)} = q_N \rho^{(k)} \cos \theta_1^{(k)}, \quad (4.2.39)$$

$$0^\circ \leq \theta_i^{(k)} \leq 90^\circ, \quad i=1, 2, \dots, N-1.$$

For each of the 2^N quadrants, we choose randomly a set of n_r values of $\Theta^{(k)} = (\theta_1^{(k)}, \theta_2^{(k)}, \dots, \theta_{N-1}^{(k)})$, and for each chosen value of $\Theta^{(k)}$, we consider the following n_r+1 values of $\rho^{(k)}$:

$$\rho_j^{(k)} = jh, \quad j=0, 1, \dots, n_r \quad (4.2.40)$$

where $h = \phi/n_r$ and $\phi^2 = \chi_{N,0.01}^2$ is the 99% point of the chi square distribution with N degrees of freedom. For each $\Theta^{(k)}$ and $\rho^{(k)}$, we use Eq.(4.2.35)-(4.2.39) to compute $(e_1^{(k)}, e_2^{(k)}, \dots, e_N^{(k)})$. We next compute $(v_1^{*(k)}, v_2^{*(k)}, \dots, v_N^{*(k)})$ using

$$\mathbf{v}_i^{*(k)} = \begin{cases} \lambda_{i1}e_i^{(k)} + \lambda_{i2}([e_i^{(k)}]^2 - (\frac{1+\lambda_{i3}}{2})), & e_i^{(k)} \geq 0 \\ \lambda_{i1}e_i^{(k)} + \lambda_{i2}(\lambda_{i3}[e_i^{(k)}]^2 - (\frac{1+\lambda_{i3}}{2})), & e_i^{(k)} < 0 \end{cases} \quad (4.2.41)$$

where $(\lambda_{i1}, \lambda_{i2}, \lambda_{i3})^T$ as defined in Section 2.4, is the parameter λ_i of the quadratic-normal distribution for $v_i^{*(k)}$.

We next compute (see Eq.(2.4.1) and (2.4.2))

$$\mathbf{w}^{*(k)} = \mathbf{B}\mathbf{v}^{*(k)}, \quad (4.2.42)$$

and

$$x_i^{(k)} = S_i^{(k)}(\text{conditioned on } S_i^{(k-1)}) = S_i^{(k-1)}(1 + r\Delta t + \sigma_i w_i^{*(k)}\sqrt{\Delta t}), \text{ for } i = 1, 2, \dots, N. \quad (4.2.43)$$

Then we find $\tilde{\mathbf{v}}^{(k)} = \tilde{\mathbf{B}}^{(k)T}(\mathbf{x}^{(k)} - \tilde{\boldsymbol{\mu}}^{(k)})$ (see Eq. (2.4.4)), and $(\tilde{e}_1^{(k)}, \tilde{e}_2^{(k)}, \dots, \tilde{e}_N^{(k)})$ (see Eq.(4.2.6)), and obtain $\tilde{\rho}^{(k)}, \tilde{\theta}_1^{(k)}, \tilde{\theta}_2^{(k)}, \dots, \tilde{\theta}_{N-1}^{(k)}$ using Eq.(4.2.15)-(4.2.20) with k^* changed to k .

From $\tilde{\Theta}^{(k)} = (\tilde{\theta}_1^{(k)}, \tilde{\theta}_2^{(k)}, \dots, \tilde{\theta}_{N-1}^{(k)})$, we find the quadrant which contains $\tilde{\Theta}^{(k)}$ and use Eq.(4.2.24) to get $\tilde{c}_g^{(k)}$, $g = 0, 1, 2$. From $\tilde{c}_g^{(k)}$, $g = 0, 1, 2$, we find

$$Q(t_k, \mathbf{x}^{(k)}) = [\tilde{c}_0^{(k)} + \tilde{c}_1^{(k)}\tilde{\rho}^{(k)} + \tilde{c}_2^{(k)}[\tilde{\rho}^{(k)}]^2]^+ \quad (4.2.44)$$

In short for a given value of $(q_1, q_2, \dots, q_N, \theta_1^{(k)}, \theta_2^{(k)}, \dots, \theta_{N-1}^{(k)})$ and the values $\rho_j^{(k)}$, $j = 0, 1, 2, \dots, \ell$ of $\rho^{(k)}$, we find $\ell + 1$ corresponding values of $Q(t_k, \mathbf{x}^{(k)})$. From these $\ell + 1$ values of $Q(t_k, \mathbf{x}^{(k)})$, we use a regression procedure to obtain

$$Q(t_k, \mathbf{x}^{(k)}) = \begin{cases} c_0^{(k)} + c_1^{(k)}\rho^{(k)} + c_2^{(k)}[\rho^{(k)}]^2, & 0 \leq \rho^{(k)} \leq \xi^{(k)} \\ 0, & \rho^{(k)} > \xi^{(k)} \end{cases} \quad (4.2.45)$$

For a given value of (q_1, q_2, \dots, q_N) , we need to compute the multiple integral

$$I_{q_1 q_2 \dots q_N} = \int_{\theta_1^{(k)}=0}^{\Pi/2} \int_{\theta_2^{(k)}=0}^{\Pi/2} \dots \int_{\theta_{N-1}^{(k)}=0}^{\Pi/2} \int_{\rho^{(k)}=0}^{\xi^{(k)}} (2\Pi)^{-(N/2)} (c_0^{(k)} + c_1^{(k)} \rho^{(k)} + c_2^{(k)} [\rho^{(k)}]^2) e^{-(1/2)[\rho^{(k)}]^2} |J| d\rho^{(k)} d\theta_{N-1}^{(k)} \dots d\theta_2^{(k)} d\theta_1^{(k)}, \quad (4.2.46)$$

where $J = [\text{Jacobian obtained from } (e_1^{(k)}, e_2^{(k)}, \dots, e_N^{(k)})] = \begin{vmatrix} \frac{\partial e_1^{(k)}}{\partial \rho^{(k)}} & \frac{\partial e_2^{(k)}}{\partial \rho^{(k)}} & \dots & \frac{\partial e_N^{(k)}}{\partial \rho^{(k)}} \\ \frac{\partial e_1^{(k)}}{\partial \theta_1^{(k)}} & \frac{\partial e_2^{(k)}}{\partial \theta_1^{(k)}} & \dots & \frac{\partial e_N^{(k)}}{\partial \theta_1^{(k)}} \\ \vdots & \vdots & \ddots & \vdots \\ \frac{\partial e_1^{(k)}}{\partial \theta_{N-1}^{(k)}} & \frac{\partial e_2^{(k)}}{\partial \theta_{N-1}^{(k)}} & \dots & \frac{\partial e_N^{(k)}}{\partial \theta_{N-1}^{(k)}} \end{vmatrix}.$

To compute the integral in Eq.(4.2.46) we

- (i) use numerical integration to perform the integration with respect to $\rho^{(k)}$.
- (ii) regress the value from (i) on $\theta_1^{(k)}, \theta_2^{(k)}, \dots, \theta_{N-1}^{(k)}$ to obtain a polynomial of low degree in the polar angles.
- (iii) use numerical integration to evaluate integrals of which the integrands are products of the powers, sines and cosines of the polar angles.

Then

$$E^* [Q(t_k, \mathbf{S}^{(k)} | \mathbf{S}^{(k-1)} = \mathbf{x}^{(k-1)})] = \sum_{q_1 = -1, +1} \sum_{q_2 = -1, +1} \dots \sum_{q_N = -1, +1} I_{q_1 q_2 \dots q_N} \quad (4.2.47)$$

and

$$Q(t_{k-1}, \mathbf{x}^{(k-1)}) = \max(h(t_{k-1}, \mathbf{x}^{(k-1)}), e^{(-r\Delta t)} E^* [Q(t_k, \mathbf{S}^{(k)} | \mathbf{S}^{(k-1)} = \mathbf{x}^{(k-1)})]). \quad (4.2.48)$$

For each of $\tilde{\Theta}^{(k-1)}$, we may approximate $Q(t_{k-1}, \mathbf{x}^{(k-1)})$ by a quadratic function of $\tilde{\rho}^{(k-1)}$ and express $Q(t_{k-1}, \mathbf{x}^{(k-1)})$ as

$$Q(t_{k-1}, \mathbf{x}^{(k-1)}) = \begin{cases} \tilde{c}_0^{(k-1)} + \tilde{c}_1^{(k-1)} \tilde{\rho}^{(k-1)} + \tilde{c}_2^{(k-1)} [\tilde{\rho}^{(k-1)}]^2, & 0 \leq \tilde{\rho}^{(k-1)} \leq \tilde{\xi}^{(k-1)} \\ 0, & \tilde{\rho}^{(k-1)} > \tilde{\xi}^{(k-1)} \end{cases} \quad (4.2.49)$$

where $\tilde{c}_0^{(k-1)}$, $\tilde{c}_1^{(k-1)}$, $\tilde{c}_2^{(k-1)}$, and $\tilde{\xi}_5^{(k-1)}$ are constants which depend on $\tilde{\Theta}^{(k-1)}$.

Examples of the fitted quadratic function of $Q(t_{k^*-1}, \mathbf{x}^{(k^*-1)})$ when $N = 3$ and $k^* = 10$ are shown in Figures 4.2.9 – 4.2.10. Figures 4.2.9 and 4.2.10 show that the right side of Eq.(4.2.49) gives a satisfy fit to the computed values of $Q(t_{k^*-1}, \mathbf{x}^{(k^*-1)})$.

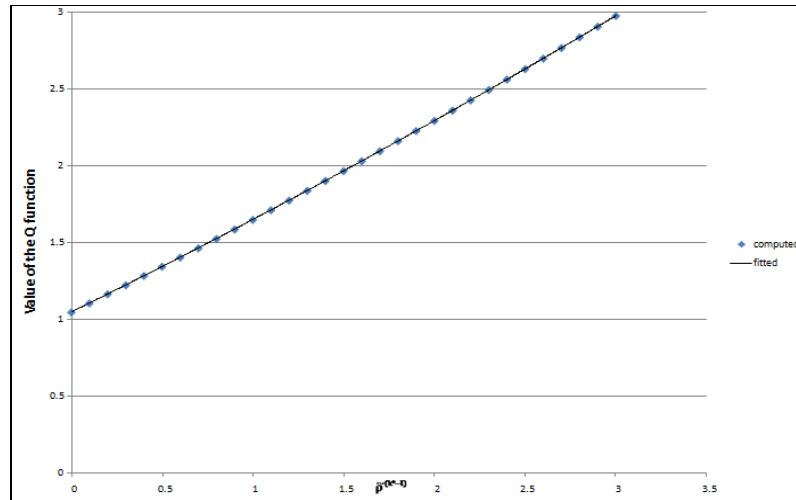


Figure 4.2.9: Computed and fitted values of $Q(t_{k^*-1}, \mathbf{x}^{(k^*-1)})$

[$N=3$, Quadrant number=1, $k^*=10$, exercise dates are 1/365, 2/365, ..., 10/365, $r=0.05$, $K=46$, $(\tilde{\theta}_1^{(k^*-1)}, \tilde{\theta}_2^{(k^*-1)}) = (40^\circ, 81^\circ)$, $(n_v, n_r) = (20, 30)$, fitted function is $y=0.02122x^2+0.58117x+1.04828$, other parameters are as given in Tables 4.2.2 and 4.2.3]

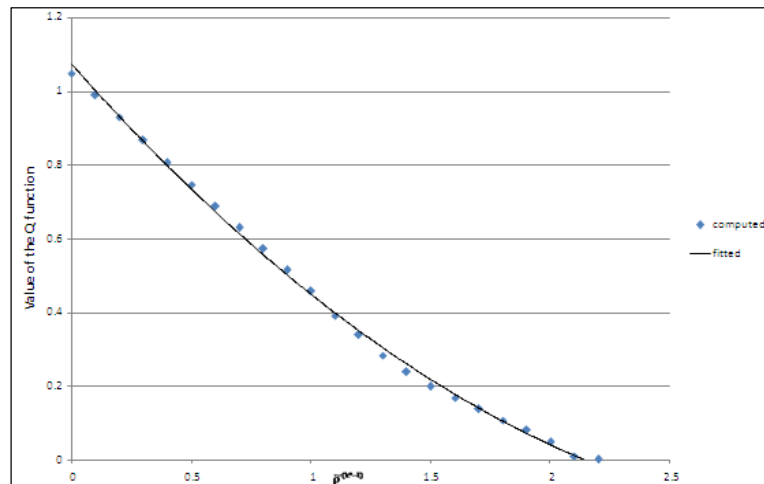


Figure 4.2.10: Computed and fitted values of $Q(t_{k-1}, \mathbf{x}^{(k-1)})$

[$N=3$, Quadrant number=5, $k^*=10$, exercise dates are 1/365, 2/365, ..., 10/365, $r=0.05\%$, $K=46$, $(\tilde{\theta}_1^{(k^*-1)}, \tilde{\theta}_2^{(k^*-1)}) = (5^\circ, 15^\circ)$, $(n_v, n_r) = (20, 30)$, fitted function is $y=0.116x^2-0.746x+1.076$, other parameters are as given in Tables 4.2.2 and 4.2.3]

Then, for each quadrant and each value of $g = 0, 1, 2$, we may regress $\tilde{c}_g^{(k-1)}$ on

$\tilde{\theta}_1^{(k-1)}, \tilde{\theta}_2^{(k-1)}, \dots, \tilde{\theta}_{N-1}^{(k-1)}$ to get

$$\tilde{c}_g^{(k-1)} = \tilde{d}_{g0}^{(k-1)} + \sum_{i=1}^{N-1} \tilde{d}_{gi}^{(k-1)} \tilde{\theta}_i^{(k-1)} + \sum_{\substack{i=1 \\ i \neq j}}^{N-1} \sum_{j=1}^{N-1} \tilde{d}_{gij}^{(k-1)} \tilde{\theta}_i^{(k-1)} \tilde{\theta}_j^{(k-1)} + \sum_{i=1}^{N-1} \tilde{d}_{gii}^{(k-1)} [\tilde{\theta}_i^{(k-1)}]^2, \quad (4.2.50)$$

for $0^\circ \leq \tilde{\theta}_i^{(k-1)} \leq 90^\circ$ and $i, j = 1, 2, \dots, N-1$.

Examples of the computed and fitted value of $\tilde{c}_g^{(k^*-1)}$, $g = 0, 1, 2$, in the first and eighth quadrants when $N = 3$ and $k^* = 10$ are shown in Figures 4.2.11 – 4.2.16. Figures 4.2.11 – 4.2.16 indicate that the right side of Eq.(4.2.50) also gives a fairly satisfactory fit to the computed values of $\tilde{c}_g^{(k^*-1)}$, $g = 0, 1, 2$.

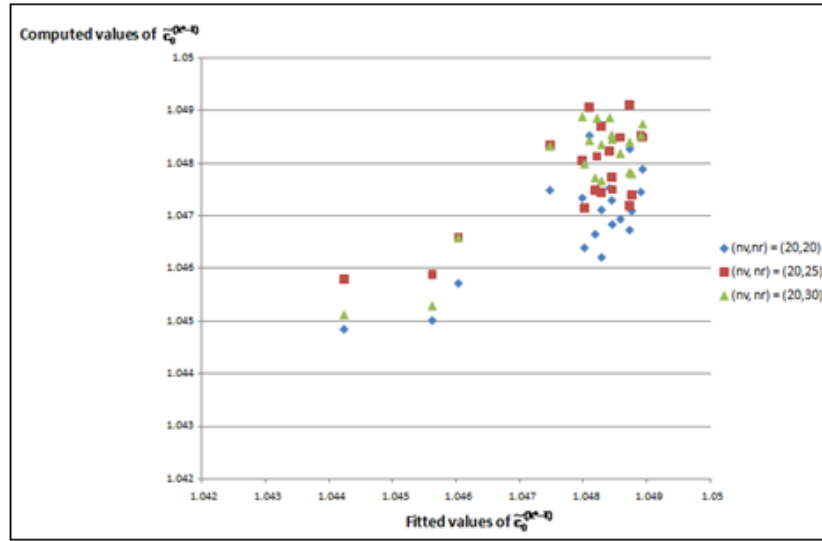


Figure 4.2.11: The fitted and computed values of the coefficient $\tilde{c}_0^{(k^*-1)}$ of $Q(t_{k^*-1}, \mathbf{x}^{(k^*-1)})$

[$N=3$, Quadrant number=1, $k^*=10$, exercise dates are $1/365, 2/365, \dots, 10/365$, $r=0.05$,

$K=46$, $(n_v, n_r)=(20, 20), (20, 25), (20, 30)$, the fitted equations for $\tilde{c}_0^{(k^*-1)}$ is

$$\begin{aligned} \tilde{c}_0^{(k^*-1)} = & 1.048 + (4.62E-05)\tilde{\theta}_1^{(k^*-1)} + (5.71E-06)\tilde{\theta}_2^{(k^*-1)} - (4.76E-7)\tilde{\theta}_1^{(k^*-1)}\tilde{\theta}_2^{(k^*-1)} \\ & - (6.28E-07)[\tilde{\theta}_1^{(k^*-1)}]^2 - (4.41E-08)[\tilde{\theta}_2^{(k^*-1)}]^2, \text{ other parameters are as given in Tables} \\ & \text{4.2.2 and 4.2.3]} \end{aligned}$$

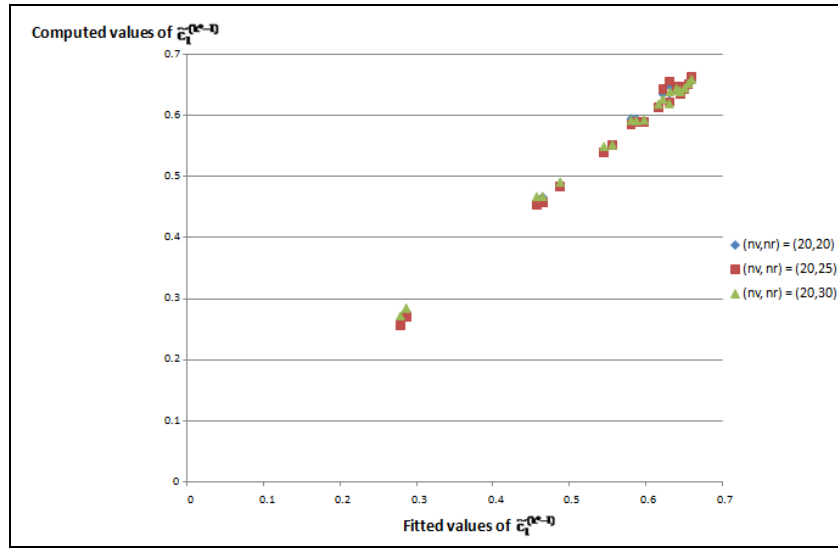


Figure 4.2.12: The fitted and computed values of the coefficient $\tilde{c}_1^{(k^*-1)}$ of $Q(t_{k^*-1}, \mathbf{x}^{(k^*-1)})$ [$N=3$, Quadrant number=1, $k^*=10$, exercise dates are $1/365, 2/365, \dots, 10/365$, $r=0.05$, $K=46$, $(n_v, n_r)=(20, 20), (20, 25), (20, 30)$, the fitted equations for $\tilde{c}_1^{(k^*-1)}$ is
$$\tilde{c}_1^{(k^*-1)} = 0.619 + 0.00309\tilde{\theta}_1^{(k^*-1)} + (8.58E - 04)\tilde{\theta}_2^{(k^*-1)} - (3.68E - 06)\tilde{\theta}_1^{(k^*-1)}\tilde{\theta}_2^{(k^*-1)} - (7.97E - 05)[\tilde{\theta}_1^{(k^*-1)}]^2 - (1.22E - 05)[\tilde{\theta}_2^{(k^*-1)}]^2$$
, other parameters are as given in Tables 4.2.2 and 4.2.3]

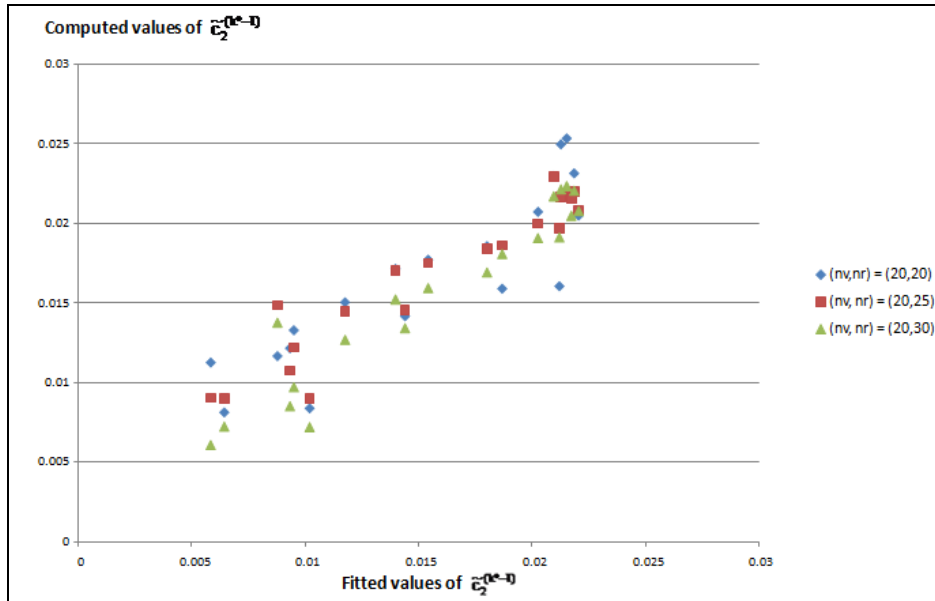


Figure 4.2.13: The fitted and computed values of the coefficient $\tilde{c}_2^{(k^*-1)}$ of $Q(t_{k^*-1}, \mathbf{x}^{(k^*-1)})$ [$N=3$, Quadrant number=1, $k^*=10$, exercise dates are $1/365, 2/365, \dots, 10/365$, $r=0.05$, $K=46$, $(n_v, n_r)=(20, 20), (20, 25), (20, 30)$, the fitted equations for $\tilde{c}_2^{(k^*-1)}$ is
$$\tilde{c}_2^{(k^*-1)} = 0.0218 - (1.83E - 04)\tilde{\theta}_1^{(k^*-1)} + (2.63E - 05)\tilde{\theta}_2^{(k^*-1)} + (1.85E - 06)\tilde{\theta}_1^{(k^*-1)}\tilde{\theta}_2^{(k^*-1)} - (1.21E - 06)[\tilde{\theta}_1^{(k^*-1)}]^2 - (2.21E - 07)[\tilde{\theta}_2^{(k^*-1)}]^2$$
, other parameters are as given in Tables 4.2.2 and 4.2.3]

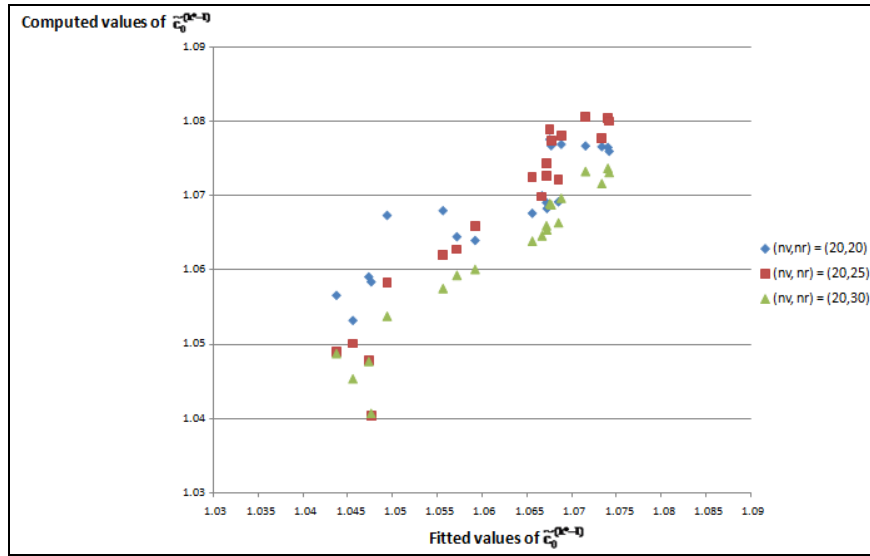


Figure 4.2.14: The fitted and computed values of the coefficient $\tilde{c}_0^{(k^*-1)}$ of $Q(t_{k^*-1}, \mathbf{x}^{(k^*-1)})$

[N=3, Quadrant number=8, $k^*=10$, exercise dates are 1/365, 2/365, ..., 10/365, $r=0.05$,

$K=46$, $(n_v, n_r)=(20, 20), (20, 25), (20, 30)$, the fitted equations for $\tilde{c}_0^{(k^*-1)}$ is

$$\begin{aligned} \tilde{c}_0^{(k^*-1)} = & 1.069 + (1.86E - 04)\tilde{\theta}_1^{(k^*-1)} + (1.77E - 04)\tilde{\theta}_2^{(k^*-1)} + (4.37E - 07)\tilde{\theta}_1^{(k^*-1)}\tilde{\theta}_2^{(k^*-1)} \\ & - (6.96E - 06)[\tilde{\theta}_1^{(k^*-1)}]^2 - (2.09E - 06)[\tilde{\theta}_2^{(k^*-1)}]^2, \text{ other parameters are as given in Tables} \\ & \text{4.2.2 and 4.2.3]} \end{aligned}$$

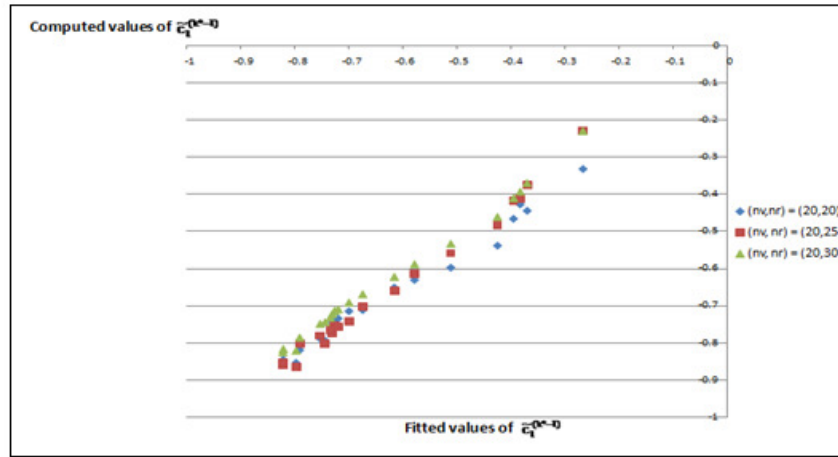


Figure 4.2.15: The fitted and computed values of the coefficient $\tilde{c}_1^{(k^*-1)}$ of $Q(t_{k^*-1}, \mathbf{x}^{(k^*-1)})$

[N=3, Quadrant number=8, $k^*=10$, exercise dates are 1/365, 2/365, ..., 10/365, $r=0.05$, $K=46$, $(n_v, n_r)=(20, 20), (20, 25), (20, 30)$, the fitted equations for $\tilde{c}_1^{(k^*-1)}$ is

$$\begin{aligned} \tilde{c}_1^{(k^*-1)} = & -0.7436 - 0.0043\tilde{\theta}_1^{(k^*-1)} - (2.90E - 03)\tilde{\theta}_2^{(k^*-1)} + (4.58E - 06)\tilde{\theta}_1^{(k^*-1)}\tilde{\theta}_2^{(k^*-1)} \\ & + (1.25E - 04)[\tilde{\theta}_1^{(k^*-1)}]^2 + (3.50E - 05)[\tilde{\theta}_2^{(k^*-1)}]^2, \text{ other parameters are as given in Tables} \\ & \text{4.2.2 and 4.2.3]} \end{aligned}$$

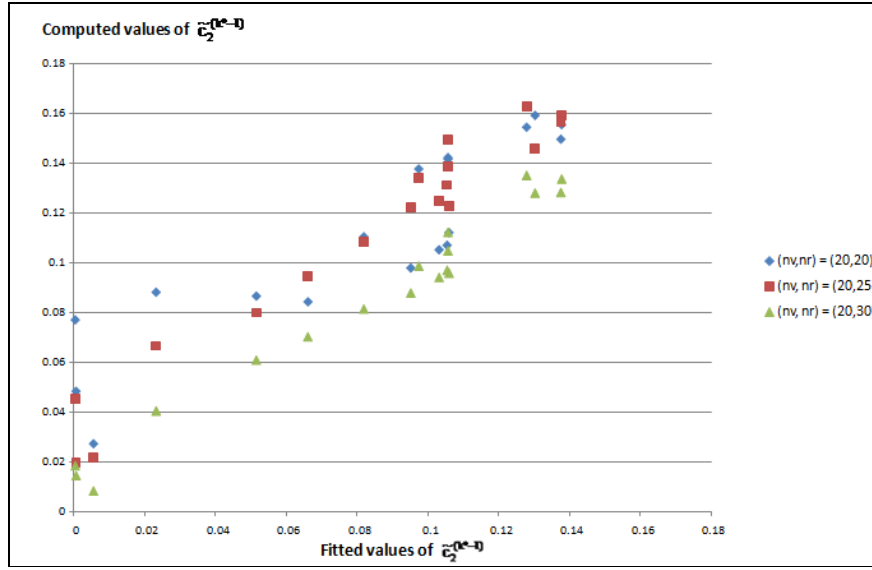


Figure 4.2.16: The fitted and computed values of the coefficient $\tilde{c}_2^{(k^*-1)}$ of $Q(t_{k^*-1}, \mathbf{x}^{(k^*-1)})$

[N=3, Quadrant number=8, $k^*=10$, exercise dates are $1/365, 2/365, \dots, 10/365$, $r=0.05$,

$K=46$, $(n_v, n_r)=(20, 20), (20, 25), (20, 30)$, the fitted equations for $\tilde{c}_2^{(k^*-1)}$ is

$$\begin{aligned} \tilde{c}_2^{(k^*-1)} = & 0.1122 + (6.81E - 04)\tilde{\theta}_1^{(k^*-1)} + (1.09E - 03)\tilde{\theta}_2^{(k^*-1)} - (3.50E - 06)\tilde{\theta}_1^{(k^*-1)}\tilde{\theta}_2^{(k^*-1)} \\ & - (2.89E - 05)[\tilde{\theta}_1^{(k^*-1)}]^2 - (1.22E - 05)[\tilde{\theta}_2^{(k^*-1)}]^2, \text{ other parameters are as given in Tables} \\ & \text{4.2.2 and 4.2.3]} \end{aligned}$$

By finding $Q(t_{k^*}, \mathbf{x}^{(k^*)}), Q(t_{k^*-1}, \mathbf{x}^{(k^*-1)}), \dots, Q(t_1, \mathbf{x}^{(1)}), Q(t_0, \mathbf{x}^{(0)})$ in the indicated order, we can finally obtain the price of the American basket call option

$$Q = Q(t_0, \mathbf{x}^{(0)}) = Q(0, \mathbf{S}(0)). \quad (4.2.51)$$

4.3 Pricing of American call options using simulation

For each of the 2^N quadrants, we choose randomly a set of n_v values of

$\tilde{\Theta}^{(k^*)} = (\tilde{\theta}_1^{(k^*)}, \tilde{\theta}_2^{(k^*)}, \dots, \tilde{\theta}_{N-1}^{(k^*)})$, and for each chosen value of $\tilde{\Theta}^{(k^*)}$, we consider the

following n_r+1 values of $\tilde{\rho}^{(k^*)}$:

$$\tilde{\rho}_j^{(k^*)} = jh, j=0, 1, \dots, n_r \quad (4.3.1)$$

where $h = \phi/n_r$ and $\phi^2 = \chi_{N,0.01}^2$ is the 99% point of the chi square distribution with N degrees of freedom. For each $\tilde{\Theta}^{(k^*)}$, we

(i) find $\tilde{e}_i^{(k^*)}$, for $i=1, 2, \dots, N$ by using Eq.(4.2.16) – (4.2.20) with $\tilde{\rho}^{(k^*)} = \tilde{\rho}_j^{(k^*)}$,

(ii) find $\tilde{v}_i^{(k^*)}$, for $i = 1, 2, \dots, N$ by using Eq.(4.2.6),

(iii) find $\mathbf{S}^{(k^*)}$ by using Eq.(4.2.5),

and

(iv) find $Q(t_{k^*}, \mathbf{x}^{(k^*)})$ using Eq.(4.2.4).

For each $\tilde{\Theta}^{(k^*)}$, we may approximate $Q(t_{k^*}, \mathbf{x}^{(k^*)})$ by a quadratic function of $\tilde{\rho}^{(k^*)}$ and express $Q(t_{k^*}, \mathbf{x}^{(k^*)})$ as

$$Q(t_{k^*}, \mathbf{x}^{(k^*)}) = \begin{cases} \tilde{c}_0^{(k^*)} + \tilde{c}_1^{(k^*)} \tilde{\rho}^{(k^*)} + \tilde{c}_2^{(k^*)} [\tilde{\rho}^{(k^*)}]^2, & 0 \leq \tilde{\rho}^{(k^*)} \leq \tilde{\xi}^{(k^*)} \\ 0, & \tilde{\rho}^{(k^*)} > \tilde{\xi}^{(k^*)} \end{cases} \quad (4.3.2)$$

where $\tilde{c}_0^{(k^*)}$, $\tilde{c}_1^{(k^*)}$, $\tilde{c}_2^{(k^*)}$ and $\tilde{\xi}^{(k^*)}$ are constants which depend on $\tilde{\Theta}^{(k^*)}$.

Then, for each quadrant and each value of $g = 0, 1, 2$, we may regress $\tilde{c}_g^{(k^*)}$ on $\tilde{\theta}_1^{(k^*)}, \tilde{\theta}_2^{(k^*)}, \dots, \tilde{\theta}_{N-1}^{(k^*)}$ to get

$$\tilde{c}_g^{(k^*)} = \tilde{d}_{g0}^{(k^*)} + \sum_{i=1}^{N-1} \tilde{d}_{gi}^{(k^*)} \tilde{\theta}_i^{(k^*)} + \sum_{i=1}^{N-1} \sum_{\substack{j=1 \\ i \neq j}}^{N-1} \tilde{d}_{gij}^{(k^*)} \tilde{\theta}_i^{(k^*)} \tilde{\theta}_j^{(k^*)} + \sum_{i=1}^{N-1} \tilde{d}_{gii}^{(k^*)} [\tilde{\theta}_i^{(k^*)}]^2, \quad (4.3.3)$$

for $0^\circ \leq \tilde{\theta}_i^{(k^*)} \leq 90^\circ$, $i, j = 1, 2, \dots, N-1$.

For $k = k^*, k^* - 1, \dots, 2, 1$, we next find $Q(t_{k-1}, \mathbf{x}^{(k-1)})$. For each of the 2^N quadrants, we choose randomly a set of n_v values of $\tilde{\Theta}^{(k-1)} = (\tilde{\theta}_1^{(k-1)}, \tilde{\theta}_2^{(k-1)}, \dots, \tilde{\theta}_{N-1}^{(k-1)})$, and for each chosen value of $\tilde{\Theta}^{(k-1)}$, we consider the following $n_r + 1$ values of $\tilde{\rho}^{(k-1)}$:

$$\tilde{\rho}_j^{(k-1)} = jh, j=0, 1, \dots, n_r \quad (4.3.4)$$

where $h = \phi/n_r$ and $\phi^2 = \chi_{N,0.01}^2$ is the 99% point of the chi square distribution with N degrees of freedom. For each $\tilde{\Theta}^{(k-1)}$, we

- (i) find $\tilde{e}_i^{(k-1)}$, for $i=1, 2, \dots, N$ by using Eq.(4.2.28) – (4.2.32) with $\tilde{\rho}^{(k-1)} = \tilde{\rho}_j^{(k-1)}$,
- (ii) find $\tilde{v}_i^{(k-1)}$, for $i=1, 2, \dots, N$ by using Eq.(4.2.26), and
- (iii) find $\mathbf{S}(t_{k-1}) = \mathbf{x}^{(k-1)}$ by using Eq.(4.2.25).

We next need to find $h(t_{k-1}, \mathbf{x}^{(k-1)})$ and $E^*[Q(t_k, \mathbf{S}^{(k)} | \mathbf{S}^{(k-1)} = \mathbf{x}^{(k-1)})]$ in order to determine $Q(t_{k-1}, \mathbf{x}^{(k-1)})$.

To find $E^*[Q(t_k, \mathbf{S}^{(k)} | \mathbf{S}^{(k-1)} = \mathbf{x}^{(k-1)})]$ using simulation, we first generate n_s values of $(e_1^{(k)}, e_2^{(k)}, \dots, e_N^{(k)})$ where $e_i^{(k)} \sim N(0,1)$ and $e_i^{(k)}$ and $e_j^{(k)}$ are uncorrelated for $i \neq j$. For each generated $(e_1^{(k)}, e_2^{(k)}, \dots, e_N^{(k)})$ we compute the corresponding $(v_1^{*(k)}, v_2^{*(k)}, \dots, v_N^{*(k)})$, $(w_1^{*(k)}, w_2^{*(k)}, \dots, w_N^{*(k)})$ and $(x_1^{(k)}, x_2^{(k)}, \dots, x_N^{(k)})$ (see Eq.(4.2.41) – (4.2.43)). We then

- (i) find $(\tilde{v}_1^{(k)}, \tilde{v}_2^{(k)}, \dots, \tilde{v}_N^{(k)})$ using Eq.(2.4.4),
- (ii) find $(\tilde{e}_1^{(k)}, \tilde{e}_2^{(k)}, \dots, \tilde{e}_N^{(k)})$ using Eq.(4.2.6) with k^* changed to k , and
- (iii) find $\tilde{\rho}^{(k)}, \tilde{\theta}_1^{(k)}, \tilde{\theta}_2^{(k)}, \dots, \tilde{\theta}_{N-1}^{(k)}$ using Eq. (4.2.15)-(4.2.20) with k^* changed to k .

From $\tilde{\Theta}^{(k)} = (\tilde{\theta}_1^{(k)}, \tilde{\theta}_2^{(k)}, \dots, \tilde{\theta}_{N-1}^{(k)})$, we find the quadrant which contains $\tilde{\Theta}^{(k)}$ and use Eq.(4.3.3) with k^* replaced by k to get $\tilde{c}_g^{(k)}$, $g = 0, 1, 2$. From $\tilde{c}_g^{(k)}$, $g = 0, 1, 2$, we find

$$Q(t_k, \mathbf{x}^{(k)}) = [\tilde{c}_0^{(k)} + \tilde{c}_1^{(k)} \tilde{\rho}^{(k)} + \tilde{c}_2^{(k)} [\tilde{\rho}^{(k)}]^2]^+ \quad (4.3.5)$$

Based on the resulting n_s values of $Q(t_k, \mathbf{x}^{(k)})$, we find the average value of $Q(t_k, \mathbf{x}^{(k)})$ and use it to estimate $E^*[Q(t_k, \mathbf{S}^{(k)} | \mathbf{S}^{(k-1)} = \mathbf{x}^{(k-1)})]$.

Then

$$Q(t_{k-1}, \mathbf{x}^{(k-1)}) = \max(h(t_{k-1}, \mathbf{x}^{(k-1)}), e^{(-r\Delta t)} E^*[Q(t_k, \mathbf{S}^{(k)} | \mathbf{S}^{(k-1)} = \mathbf{x}^{(k-1)})]). \quad (4.3.6)$$

For each of $\tilde{\Theta}^{(k-1)}$, we may approximate $Q(t_{k-1}, \mathbf{x}^{(k-1)})$ by a quadratic function of $\tilde{\rho}^{(k-1)}$ and express $Q(t_{k-1}, \mathbf{x}^{(k-1)})$ as

$$Q(t_{k-1}, \mathbf{x}^{(k-1)}) = \begin{cases} \tilde{c}_0^{(k-1)} + \tilde{c}_1^{(k-1)} \tilde{\rho}^{(k-1)} + \tilde{c}_2^{(k-1)} [\tilde{\rho}^{(k-1)}]^2, & 0 \leq \tilde{\rho}^{(k-1)} \leq \tilde{\xi}^{(k-1)} \\ 0, & \tilde{\rho}^{(k-1)} > \tilde{\xi}^{(k-1)} \end{cases} \quad (4.3.7)$$

where $\tilde{c}_0^{(k-1)}$, $\tilde{c}_1^{(k-1)}$, $\tilde{c}_2^{(k-1)}$, and $\tilde{\xi}^{(k-1)}$ are constants which depend on $\tilde{\Theta}^{(k-1)}$.

Then, for each quadrant and each value of $g = 0, 1, 2$, we may regress $\tilde{c}_g^{(k-1)}$ on

$\tilde{\theta}_1^{(k-1)}, \tilde{\theta}_2^{(k-1)}, \dots, \tilde{\theta}_{N-1}^{(k-1)}$ to get

$$\tilde{c}_g^{(k-1)} = \tilde{d}_{g0}^{(k-1)} + \sum_{i=1}^{N-1} \tilde{d}_{gi}^{(k-1)} \tilde{\theta}_i^{(k-1)} + \sum_{\substack{i=1 \\ i \neq j}}^{N-1} \sum_{j=1}^{N-1} \tilde{d}_{gij}^{(k-1)} \tilde{\theta}_i^{(k-1)} \tilde{\theta}_j^{(k-1)} + \sum_{i=1}^{N-1} \tilde{d}_{gii}^{(k-1)} [\tilde{\theta}_i^{(k-1)}]^2, \quad (4.3.8)$$

for $0^\circ \leq \tilde{\theta}_i^{(k-1)} \leq 90^\circ$ and $i, j = 1, 2, \dots, N-1$.

By finding $Q(t_{k^*}, \mathbf{x}^{(k^*)}), Q(t_{k^*-1}, \mathbf{x}^{(k^*-1)}), \dots, Q(t_1, \mathbf{x}^{(1)}), Q(t_0, \mathbf{x}^{(0)})$ in the indicated order, we can finally obtain the price of the American basket call option,

$$Q = Q(t_0, \mathbf{x}^{(0)}) = Q(0, \mathbf{S}(0)). \quad (4.3.9)$$

We note the procedure in this section is similar to that given in Section 4.2. The main difference is that instead of using numerical integration to compute the conditional expectation $E^*[Q(t_k, \mathbf{S}^{(k)} | \mathbf{S}^{(k-1)} = \mathbf{x}^{(k-1)})]$ in Section 4.2 (see Eq.(4.2.46), (4.2.47) and (4.2.48)), we use simulation in this section to estimate the same conditional expectation.

4.4 Numerical examples

Case A: Pricing American call options when N=3

Let $K=46$, $a_1=0.3$, $a_2=0.3$, and $a_3=0.4$. Suppose the (i, j) entry of $\mathbf{P} = \{\text{corr}(w_i^{(k)}, w_j^{(k)})\}$ is given by Table 4.2.2 and consider four sets of values of $\mu_i, \sigma_i, \mathbf{S}^{(0)}$, $i=1, 2, 3$ given by Table 4.4.1. The results for the American call option prices for $k^*=10$ and 30 are shown in Table 4.4.2 and Table 4.4.4 respectively. The computing times required for computing the American call option prices for $k^* = 10$ and 30 by using numerical method and simulation (in minutes) in an Intel(R) Core(TM) i5 processor 2.27GHz computer are shown in Table 4.4.3 and Table 4.4.5 respectively.

Table 4.4.1: Values of $\mu_i, \sigma_i, \mathbf{S}^{(0)}$, $\bar{m}_3^{(i)}$ and $\bar{m}_4^{(i)}$

[Number of underlying assets is $N=3$, $r=0.05$, $K=46$, $a_1=0.3$, $a_2=0.3$, $a_3=0.4$]

Example	i	μ_i	σ_i	$\mathbf{S}^{(0)}$	$\bar{m}_3^{(i)}$	$\bar{m}_4^{(i)}$
A ₁	1	0.05	0.15	50	0.0	3.0
	2	0.05	0.1	60	0.0	3.0
	3	0.05	0.2	35	0.0	3.0
A ₂	1	0.05	0.15	50	0.0	8.0
	2	0.05	0.1	60	0.0	8.0
	3	0.05	0.2	35	0.0	8.0
A ₃	1	0.05	0.15	50	0.1	3.0
	2	0.05	0.1	60	0.1	3.0
	3	0.05	0.2	35	0.1	3.0
A ₄	1	0.05	0.15	50	0.1	5.0
	2	0.05	0.1	60	0.2	4.0
	3	0.05	0.2	35	0.2	3.8

Table 4.4.2: Results for American call option prices

[Number of underlying assets is $N = 3$, $k^*=10$, exercise dates are $1/365, 2/365, \dots, 10/365$, $r=0.05$, $K=46$, $a_1 = 0.3$, $a_2 = 0.3$, $a_3 = 0.4$, other parameters are as given in Tables 4.2.2 and 4.4.1]

Example	(n_v, n_r)	Numerical Method	Simulation	
			$n_s=1,000$	$n_s=10,000$
A ₁	(20,5)	1.07386	1.07513	1.07385
	(20,10)	1.07286	1.07377	1.07297
	(20,15)	1.07206	1.07424	1.07251
	(20,20)	1.07290	1.07396	1.07282
	(20,25)	1.07252	1.07036	1.07200
	(20,30)	1.07221	1.07447	1.07284
	(25,30)	1.07197	1.07026	1.07121
	(30,30)	1.07181	1.07285	1.07167
A ₂	(20,5)	1.40158	1.39761	1.40625
	(20,10)	1.43865	1.42870	1.43507
	(20,15)	1.44019	1.43014	1.44381
	(20,20)	1.46270	1.45508	1.46567
	(20,25)	1.46854	1.45989	1.46802
	(20,30)	1.46996	1.45751	1.46588
	(25,30)	1.46839	1.46338	1.46445
	(30,30)	1.46701	1.46031	1.46682
A ₃	(20,5)	1.18216	1.15853	1.17812
	(20,10)	1.17726	1.17046	1.17430
	(20,15)	1.19874	1.18194	1.19610
	(20,20)	1.21031	1.20543	1.21707
	(20,25)	1.21054	1.20960	1.21169
	(20,30)	1.23852	1.22629	1.23634
	(25,30)	1.24432	1.23296	1.24906
	(30,30)	1.24291	1.24015	1.24177
A ₄	(20,5)	1.72343	1.71063	1.72120
	(20,10)	1.70150	1.69207	1.70448
	(20,15)	1.77721	1.76829	1.77388
	(20,20)	1.97814	1.96577	1.97558
	(20,25)	2.11944	2.12441	2.11823
	(20,30)	2.02370	1.98887	2.02318
	(25,30)	2.11902	2.09741	2.11811
	(30,30)	2.13794	2.12675	2.13966

From Table 4.4.2 we can get the following findings:

- F₁: The American call option prices found by using numerical method agree well with those based on simulation especially when the number n_s of points chosen randomly from the N-dimensional space is very large.
- F₂: When the distributions of $v_i^{(k)}$ are normal (see example A₁ in Tables 4.4.1 and 4.4.2), an increase in the value of (n_v, n_r) does not affect the price based on numerical method very much. However when the distributions of $v_i^{(k)}$ deviate from normality (see examples A₂, A₃, and A₄ in Tables 4.4.1 and 4.4.2), the variation of n_v and n_r has a rather large effect on the price based on numerical method. Thus when the $v_i^{(k)}$ are non-normal, we need to use fairly large n_v and n_r in order to compute the price accurately.
- F_{3a}: As we move from example A₁ to A₂, the kurtosis of the distributions of $v_i^{(k)}$ increases from 3.0 to 8.0, and the American call option price also increases from about 1.07 to 1.46.
- F_{3b}: As we move from example A₁ to A₃, the skewness of the distributions of $v_i^{(k)}$ increases from 0 to 0.1, and the American call option price also increases from about 1.07 to 1.24.
- F_{3c}: When the distributions of $v_i^{(k)}$ are skewed and having larger kurtosis, the American call option price tends to deviate from the American call option price computed when the distributions of $v_i^{(k)}$ are normal.

Table 4.4.3: Computation times (in minutes) required for computing the American call option prices presented in Table 4.4.2

[Number of underlying assets is $N = 3$, $k^*=10$, exercise dates are $1/365, 2/365, \dots, 10/365$, $r=0.05$, $K=46$, $a_1 = 0.3$, $a_2 = 0.3$, $a_3 = 0.4$, other parameters are as given in Tables 4.2.2 and 4.4.1]

(n_v, n_r)	Numerical Method	Simulation	
		$n_s=1,000$	$n_s=10,000$
(20,5)	4.68	3.54	5.14
(20,10)	6.38	6.21	9.32
(20,15)	9.85	9.54	13.45
(20,20)	12.61	12.45	17.67
(20,25)	16.55	16.04	21.29
(20,30)	20.75	20.57	25.02
(25,30)	25.18	25.02	30.38
(30, 30)	29.75	29.46	35.75

From Table 4.4.3 we see that the computing times required by numerical method are comparable to those required by the simulation procedure when $n_s = 1,000$. But when $n_s = 10,000$, the simulation procedure requires slightly longer time.

Table 4.4.4: Results for American call option prices

[Number of underlying assets is $N = 3$, $k^*=30$, exercise dates are $1/365, 2/365, \dots, 30/365$, $r=0.05$, $K=46$, $a_1 = 0.3$, $a_2 = 0.3$, $a_3 = 0.4$, other parameters are as given in Tables 4.2.2 and 4.4.1]

Example	(n_v, n_r)	Numerical Method	Simulation	
			$n_s=1,000$	$n_s=10,000$
A ₁	(20,5)	1.21096	1.22001	1.20630
	(20,10)	1.20050	1.21585	1.20245
	(20,15)	1.20712	1.19733	1.20456
	(20,20)	1.20064	1.19910	1.20201
	(20,25)	1.20702	1.19841	1.20380
	(20,30)	1.20237	1.20158	1.20390
	(25,30)	1.20017	1.20313	1.20189
	(30,30)	1.20580	1.20449	1.20507
A ₂	(20,5)	1.24745	1.23088	1.24698
	(20,10)	1.24016	1.23028	1.24166
	(20,15)	1.24488	1.23167	1.24568
	(20,20)	1.24836	1.24177	1.24706
	(20,25)	1.23027	1.23876	1.23190
	(20,30)	1.23964	1.23095	1.23690
	(25,30)	1.23928	1.23759	1.23858
	(30,30)	1.23450	1.23328	1.23384
A ₃	(20,5)	1.16859	1.18691	1.16428
	(20,10)	1.16985	1.16676	1.16722
	(20,15)	1.17137	1.17981	1.17083
	(20,20)	1.17453	1.17146	1.17314
	(20,25)	1.18784	1.18984	1.18997
	(20,30)	1.18675	1.18435	1.18553
	(25,30)	1.18722	1.18647	1.18823
	(30,30)	1.18609	1.18546	1.18596
A ₄	(20,5)	1.27918	1.24168	1.27849
	(20,10)	1.24114	1.25969	1.24599
	(20,15)	1.26077	1.27294	1.26162
	(20,20)	1.28836	1.25073	1.28990
	(20,25)	1.26835	1.26172	1.26230
	(20,30)	1.24990	1.24564	1.24767
	(25,30)	1.24034	1.24122	1.24350
	(30,30)	1.24178	1.24355	1.24808

From Table 4.4.4, we see that the findings F_1 , F_2 , F_{3a} , and F_{3c} derived from Table 4.4.2 basically still hold. However Table 4.4.4 shows that an increase in skewness may also result in a decrease in the American call option price.

Table 4.4.5: Computation times (in minutes) required for computing the American call option prices presented in Table 4.4.4

[Number of underlying assets is $N = 3$, $k^*=30$, exercise dates are $1/365, 2/365, \dots, 30/365$, $r=0.05$, $K=46$, $a_1 = 0.3$, $a_2 = 0.3$, $a_3 = 0.4$, other parameters are as given in Tables 4.2.2 and 4.4.1]

(n_v, n_r)	Numerical Method	Simulation	
		$n_s=1,000$	$n_s=10,000$
(20,5)	12.82	11.62	16.28
(20,10)	19.20	18.56	27.89
(20,15)	29.57	28.67	40.36
(20,20)	37.85	37.32	53.01
(20,25)	49.62	49.36	63.91
(20,30)	62.12	62.07	75.02
(25,30)	50.35	50.08	91.06
(30, 30)	89.21	89.19	107.22

From Table 4.4.5, we see that the computing times required by numerical method are comparable to those required by the simulation procedure when $n_s = 1,000$. But when $n_s = 10,000$, the simulation procedure requires longer time.

Case B: Pricing American call options when N=4

Consider the case when $K=46.5$, $a_1 = 0.2$, $a_2 = 0.3$, $a_3 = 0.2$ and $a_4 = 0.3$. Suppose the (i, j) entry of $\mathbf{P} = \{\text{corr}(w_i^{(k)}, w_j^{(k)})\}$ is given by Table 4.4.6 and consider four sets of values of $\mu_i, \sigma_i, \mathbf{S}^{(0)}$, for $i = 1, 2, 3, 4$, given by Table 4.4.7. The results for the American call option prices are shown in Table 4.4.8. The computing times required for computing the American call option prices by using numerical method and simulation (in minutes) respectively in an Intel(R) Core(TM) i5 processor 2.27GHz computer are shown in Table 4.4.9.

Table 4.4.6: The (i, j) entry of $\mathbf{P} = \{\text{corr}(w_i^{(k)}, w_j^{(k)})\}$

		j			
		1	2	3	4
i	1	1	0.01	0.045	0.08
	2	0.01	1	0.05	0.03
	3	0.045	0.05	1	0.1
	4	0.08	0.03	0.1	1

Table 4.4.7: Values of $\mu_i, \sigma_i, \mathbf{S}^{(0)}, \bar{m}_3^{(i)}$ and $\bar{m}_4^{(i)}$

[Number of underlying assets is $N=4$, $k^*=10$, exercise dates are $1/365, 2/365, \dots, 10/365$,
 $r=0.05, K=46.5, a_1 = 0.2, a_2 = 0.3, a_3 = 0.2, a_4 = 0.3$]

Example	i	μ_i	σ_i	$\mathbf{S}^{(0)}$	$\bar{m}_3^{(i)}$	$\bar{m}_4^{(i)}$
B ₁	1	0.05	0.15	50	0.0	3.0
	2	0.05	0.1	60	0.0	3.0
	3	0.05	0.2	35	0.0	3.0
	4	0.05	0.2	40	0.0	3.0
B ₂	1	0.05	0.15	50	0.0	5.0
	2	0.05	0.1	60	0.0	5.0
	3	0.05	0.2	35	0.0	5.0
	4	0.05	0.2	40	0.0	5.0
B ₃	1	0.05	0.15	50	0.1	3.0
	2	0.05	0.1	60	0.1	3.0
	3	0.05	0.2	35	0.1	3.0
	4	0.05	0.2	40	0.1	3.0
B ₄	1	0.05	0.15	50	0.1	5.0
	2	0.05	0.1	60	0.2	4.0
	3	0.05	0.2	35	0.2	3.8
	4	0.05	0.2	40	0.3	3.4

Table 4.4.8: Results for American call option prices

[Number of underlying assets is $N=4$, $k^*=10$, exercise dates are $1/365, 2/365, \dots, 10/365$, $r=0.05$, $K=46.5$, $a_1 = 0.2$, $a_2 = 0.3$, $a_3 = 0.2$, $a_4 = 0.3$, other parameters are as given in Tables 4.4.6 and 4.4.7]

Example	(n_v, n_r)	Numerical Method	Simulation	
			$n_s=1,000$	$n_s=10,000$
B ₁	(50,30)	0.72728	0.74401	0.72539
	(100,30)	0.73897	0.72578	0.73391
	(200,30)	0.74089	0.74219	0.74122
B ₂	(50,30)	0.76091	0.74009	0.75935
	(100,30)	0.76002	0.75401	0.76195
	(200,30)	0.77610	0.76046	0.77723
B ₃	(50,30)	0.73274	0.72530	0.73943
	(100,30)	0.72066	0.72747	0.72469
	(200,30)	0.72505	0.72122	0.72344
B ₄	(50,30)	0.70992	0.71447	0.70712
	(100,30)	0.70312	0.70139	0.70437
	(200,30)	0.70005	0.70734	0.70296

From Table 4.4.8, we see that the findings F_1 , F_{3a} , and F_{3c} derived from Table 4.4.2 also hold. However Table 4.4.8 shows that an increase in skewness may also result in a decrease in the American call option price.

Table 4.4.9: Computation times (in minutes) required for computing the American call option prices presented in Table 4.4.8

[Number of underlying assets is $N=4$, $k^*=10$, exercise dates are $1/365, 2/365, \dots, 10/365$, $r=0.05$, $K=46.5$, $a_1 = 0.2$, $a_2 = 0.3$, $a_3 = 0.2$, $a_4 = 0.3$, other parameters are as given in Tables 4.4.6 and 4.4.7]

(n_v, n_r)	Numerical Method	Simulation	
		$n_s=1,000$	$n_s=10,000$
(50, 30)	12.496	8.99	320.79
(100, 30)	24.867	18.01	641.78
(200, 30)	49.865	27.00	962.45

From Table 4.4.9, we see that the computing times required by numerical method are slightly longer than those required by simulation procedure when $n_s = 1,000$. But when $n_s = 10,000$, the simulation procedure requires much longer time.

Case C: Pricing American call options when N=6

Consider the case when $K=46.5$, $a_1 = 0.2$, $a_2 = 0.2$, $a_3 = 0.2$, $a_4 = 0.1$, $a_5 = 0.1$ and $a_6 = 0.2$. Suppose the (i,j) entry of $\mathbf{P} = \{\text{corr}(w_i^{(k)}, w_j^{(k)})\}$ is given by Table 4.4.10 and consider three sets of values of $\mu_i, \sigma_i, \mathbf{S}^{(0)}$ for $i = 1, 2, \dots, 6$, given by Table 4.4.11. The results for the American call option prices are shown in Table 4.4.12. The computing times required for computing the American call option prices by using numerical method and simulation (in minutes) respectively in an Intel(R) Core(TM) i5 processor 2.27GHz computer are shown in Table 4.4.13.

Table 4.4.10: The (i, j) entry of $\mathbf{P} = \{\text{corr}(w_i^{(k)}, w_j^{(k)})\}$

		j					
		1	2	3	4	5	6
i	1	1	0.01	0.045	0.08	0.05	0.1
	2	0.01	1	0.05	0.03	0.1	0.07
	3	0.045	0.05	1	0.1	0.075	0.09
	4	0.08	0.03	0.1	1	0.07	0.05
	5	0.05	0.1	0.075	0.07	1	0.04
	6	0.1	0.07	0.09	0.05	0.04	1

Table 4.4.11: Values of $\mu_i, \sigma_i, \mathbf{S}^{(0)}, \bar{m}_3^{(i)}$ and $\bar{m}_4^{(i)}$

[Number of underlying assets is $N=6$, $k^*=10$, exercise dates are $1/365, 2/365, \dots, 10/365$,
 $r=0.05$, $K=46.5$, $a_1 = 0.2$, $a_2 = 0.2$, $a_3 = 0.2$, $a_4 = 0.1$, $a_5 = 0.1$, $a_6 = 0.2$]

Example	i	μ_i	σ_i	$\mathbf{S}^{(0)}$	$\bar{m}_3^{(i)}$	$\bar{m}_4^{(i)}$
C ₁	1	0.05	0.15	50	0.0	3.0
	2	0.05	0.10	60	0.0	3.0
	3	0.05	0.20	35	0.0	3.0
	4	0.05	0.20	40	0.0	3.0
	5	0.05	0.20	45	0.0	3.0
	6	0.05	0.20	52	0.0	3.0
C ₂	1	0.05	0.15	50	0.0	5.0
	2	0.05	0.10	60	0.0	5.0
	3	0.05	0.20	35	0.0	5.0
	4	0.05	0.20	40	0.0	5.0
	5	0.05	0.20	45	0.0	5.0
	6	0.05	0.20	52	0.0	5.0
C ₃	1	0.05	0.15	50	0.1	3.6
	2	0.05	0.10	60	0.1	3.2
	3	0.05	0.20	35	0.1	3.4
	4	0.05	0.20	40	0.1	3.0
	5	0.05	0.20	45	0.1	3.8
	6	0.05	0.20	52	0.1	4.0

Table 4.4.12: Results for American call option prices

[Number of underlying assets is $N=6$, $k^*=10$, exercise dates are $1/365, 2/365, \dots, 10/365$, $r=0.05$, $K=46.5$, $a_1 = 0.2$, $a_2 = 0.2$, $a_3 = 0.2$, $a_4 = 0.1$, $a_5 = 0.1$, $a_6 = 0.2$, other parameters are as given in Tables 4.4.10 and 4.4.11]

Example	(n_v, n_r)	Numerical Method	Simulation	
			$n_s=1,000$	$n_s=10,000$
C ₁	(50,30)	1.39999	1.40089	1.40059
	(100,30)	1.39266	1.40035	1.39412
	(200,30)	1.39571	1.40201	1.39725
	(300,30)	1.39720	1.40252	1.39788
	(400,30)	1.39247	1.40003	1.39275
C ₂	(50,30)	1.39864	1.40163	1.40048
	(100,30)	1.40054	1.41781	1.40443
	(200,30)	1.40190	1.41650	1.40259
	(300,30)	1.40855	1.41030	1.40828
	(400,30)	1.40974	1.41002	1.40996
C ₃	(50,30)	1.41880	1.41012	1.41677
	(100,30)	1.41983	1.41286	1.41530
	(200,30)	1.41557	1.41027	1.41546
	(300,30)	1.41188	1.41747	1.41054
	(400,30)	1.41347	1.41019	1.41517

From Table 4.4.12, we see that the findings F_1 , F_2 and F_{3c} derived from Table 4.4.2 also hold. However Table 4.4.12 shows that an increase in kurtosis may instead result in a slight increase in the American call option price.

Table 4.4.13: Computation times (in minutes) required for computing the American call option prices presented in Table 4.4.12

[Number of underlying assets is $N=6$, $k^*=10$, exercise dates are $1/365, 2/365, \dots, 10/365$, $r=0.05$, $K=46.5$, $a_1 = 0.2$, $a_2 = 0.2$, $a_3 = 0.2$, $a_4 = 0.1$, $a_5 = 0.1$, $a_6 = 0.2$, other parameters are as given in Tables 4.4.10 and 4.4.11]

(n_v, n_r)	Numerical Method	Simulation	
		$n_s=1,000$	$n_s=10,000$
(50, 30)	120.25	135.21	1650.12
(100, 30)	253.18	270.51	3270.43
(200, 30)	1012.28	1078.36	6510.76
(300,30)	1665.15	1692.67	13030.32
(400,30)	2160.00	2241.39	26040.16

From Table 4.4.13, we see that the computing times required by numerical method are comparable to those required by simulation procedure when $n_s = 1,000$. But when $n_s = 10,000$, the simulation procedure requires much longer time.

Case D: Pricing American call options when $N=8$

Consider the case when $K=47$, $a_1 = 0.2$, $a_2 = 0.1$, $a_3 = 0.2$, $a_4 = 0.1$, $a_5 = 0.1$, $a_6 = 0.2$, $a_7 = 0.1$ and $a_8 = 0.1$. Suppose the (i, j) entry of $\mathbf{P} = \{\text{corr}(w_i^{(k)}, w_j^{(k)})\}$ is given by Table 4.4.14 and the values of $\mu_i, \sigma_i, \mathbf{S}^{(0)}$ for $i=1, 2, \dots, 8$ are given by Table 4.4.15. The results for the American call option prices are shown in Table 4.4.16. The computing times required for computing the American call option prices by using numerical integration and simulation (in minutes) respectively in an Intel(R) Core(TM) i5 processor 2.27GHz computer are shown in Table 4.4.17.

Table 4.4.14: The (i, j) entry of $\mathbf{P} = \{\text{corr}(w_i^{(k)}, w_j^{(k)})\}$

		j							
		1	2	3	4	5	6	7	8
i	1	1	0.01	0.045	0.08	0.05	0.1	0.02	0.035
	2	0.01	1	0.05	0.03	0.1	0.07	0.04	0.09
	3	0.045	0.05	1	0.1	0.075	0.09	0.1	0.07
	4	0.08	0.03	0.1	1	0.07	0.05	0.06	0.12
	5	0.05	0.1	0.075	0.07	1	0.04	0.21	0.045
	6	0.1	0.07	0.09	0.05	0.04	1	0.11	0.02
	7	0.02	0.04	0.1	0.06	0.21	0.11	1	0.05
	8	0.035	0.09	0.07	0.12	0.045	0.02	0.05	1

Table 4.4.15: Values of $\mu_i, \sigma_i, \mathbf{S}^{(0)}, \bar{m}_3^{(i)}$ and $\bar{m}_4^{(i)}$

[Number of underlying assets is $N=8$, $k^*=10$, exercise dates are $1/365, 2/365, \dots, 10/365$, $r=0.05$, $K=47$, $a_1 = 0.2$, $a_2 = 0.1$, $a_3 = 0.2$, $a_4 = 0.1$, $a_5 = 0.1$, $a_6 = 0.1$, $a_7 = 0.1$, $a_8 = 0.1$]

i	μ_i	σ_i	$\mathbf{S}^{(0)}$	$\bar{m}_3^{(i)}$	$\bar{m}_4^{(i)}$
1	0.05	0.15	50	0.0	3.0
2	0.05	0.10	60	0.0	3.0
3	0.05	0.20	35	0.0	3.0
4	0.05	0.20	40	0.0	3.0
5	0.05	0.20	45	0.0	3.0
6	0.05	0.20	52	0.0	3.0
7	0.05	0.15	50	0.0	3.0
8	0.05	0.10	60	0.0	3.0

Table 4.4.16: Results for American call option prices

[Number of underlying assets is $N=8$, $k^*=10$, exercise dates are $1/365, 2/365, \dots, 10/365$, $r=0.05$, $K=47$, $a_1 = 0.2$, $a_2 = 0.1$, $a_3 = 0.2$, $a_4 = 0.1$, $a_5 = 0.1$, $a_6 = 0.1$, $a_7 = 0.1$, $a_8 = 0.1$, other parameters are as given in Tables 4.4.14 and 4.4.15]

(n_v, n_r)	Numerical Method	Simulation	
		$n_s=1,000$	$n_s=10,000$
(50,30)	1.4544	1.4840	1.4858
(100,30)	1.4665	1.4504	1.4680
(200,30)	1.4770	1.4783	1.4786

From Table 4.4.16 we can get the following findings:

- (i) The American call option prices found by using numerical method agree fairly well with those based on simulation especially when the number n_s of points chosen randomly from the N -dimensional space is very large.
- (ii) When the distributions of $v_i^{(k)}$ are fairly normal, the value of $(n_v, n_r) = (50, 30)$ leads to a value of American call option price which is accurate up to the first decimal place. However the value of $(n_v, n_r) = (200, 30)$ is still unable to lead to a value for the American call option price which is accurate up to the second decimal place.

Table 4.4.17: Computation times (in minutes) required for computing the American call option prices presented in Table 4.4.16

[Number of underlying assets is $N=8$, $k^*=10$, exercise dates are $1/365, 2/365, \dots, 10/365$, $r=0.05$, $K=47$, $a_1 = 0.2$, $a_2 = 0.1$, $a_3 = 0.2$, $a_4 = 0.1$, $a_5 = 0.1$, $a_6 = 0.1$, $a_7 = 0.1$, $a_8 = 0.1$, other parameters are as given in Tables 4.4.14 and 4.4.15]

(n_v, n_r)	Numerical Method	Simulation	
		$n_s=1,000$	$n_s=10,000$
(50, 30)	1355.10	2040.21	6110.12
(100, 30)	7500.838	7950.84	13287.36
(200, 30)	13586.45	13712.23	18537.49

From Table 4.4.17 we see that the computing times required by numerical method are comparable with those required by the simulation procedure when $n_s = 1,000$. But when $n_s = 10,000$, the simulation procedure requires much longer time.